DETERMINATION OF OPTICAL CONSTANTS OF KTP CRYSTAL USING ELLIPSOMETRY TECHNIQUE

By

Asmamaw Molla

A Thesis

Submitted to The School of Graduate Studies of Addis Ababa University

in Partial Fulfilment of The Requirements For The Degree of

Master of Science in Physics

JUNE, 2005

ADDIS ABABA UNIVERSITY

Date: **June, 2005**

Author: **Asmamaw Molla**

Title: **DETERMINATION OF OPTICAL CONSTANTS OF KTP CRYSTAL USING ELLIPSOMETRY TECHNIQUE**

Department: **Physics**

Degree: **M.Sc.**

Permission is herewith granted to Addis Ababa University to circulate and to have copied for non-commercial purposes, at its discretion, the above title upon the request of individuals or institutions.

Signature of Author

My Parents

Acknowledgements

Words can not express my deep appreciation to Dr. A.K. Chaudhary and Dr.Araya Asfaw, my advisors, for their many suggestions and constant support during this research. Dr. A.K. Chaudhary identified the problem to be studied, supplied me the KTP crystal and many useful reference materials, shared his experimental knowledge with me, and gave constant suggestion and correction on the thesis. Dr. Areaya Asfaw allow me to work in the optical laboratory and supplied me all facilities and equipments necessary for the work. He also gave me constructive suggestions and comments before the final print out of the thesis.

Dr.Mesfin Redi expressed his interest in my work and supplied me with the prints of some of the related work which gave me a better perspective on my own results. He also shared with me his knowledge of ellipsometry technique and data analysis and provided many useful references and friendly encouragement.

I am thankful to the Department of Physics (AAU) and its staff members for constant material and moral support.

I am also thankfnl to Prof. G.C. Bhar, Department of Physics, Burdwan University, Burdwan-713104 (W.B.), India for providing KTP crystal.

Of course, I am grateful to my parents for their support and *love*. Without them this work would never have come into existence (literally).

Finally, I wish to thank the following: Tesfaye Mekonen,(for his brotherhood), Tsodoniya (for special effects); Gebregiorgis (George) Abrha, Belete Regassa and other friends of mine... (for all the good and bad times we had together).

Asmamaw Molla

June, 2005

Addis Ababa.

Table of Contents

Table of Contents vi

Abstract x

Introduction 1

1 INTERACTION OF LIGHT WITH MATTER 6
- 1.1 Maxwell's Equations . . . 6
- 1.2 Propagation of Light in Dielectric Materials . . . 7
- 1.3 Propagation of Light in a Crystal . . . 10
- 1.4 Propagation of Light Across a Plane Interface of Nonconducting (Dielectric) Materials . . . 17
  - 1.4.1 Fresnel Coefficients . . . 18
  - 1.4.2 Fabry-Perot Equations . . . 23

2 THE POLARIZATION OF LIGHT WAVES 26
- 2.1 Polarization of Monochromatic Waves of Arbitrary Spatial Structure . 27
  - 2.1.1 Elliptical Polarization . . . 27
  - 2.1.2 Linear And Circular Polarizations . . . 29
- 2.2 Jones Vector . . . 30
  - 2.2.1 The Jones Vector of a Uniform TE Plane Wave . . . 30
  - 2.2.2 Jones Vector of Some State of Polarization . . . 33
- 2.3 Jones Matrix . . . 34
  - 2.3.1 The significance of the elements T_{ij} of the Jones matrix . . . 37
  - 2.3.2 Jones matrices of reflection-type devices . . . 38

3 THEORY AND ANALYSIS OF MEASUREMENTS IN ELLIPSOMETRY SYSTEMS 40
- 3.1 Introduction . . . 40

3.2 Reflection Ellipsometry 41
3.3 Derivation of Ellipsometer Equations 42
3.4 The Principle of Operation (Methodology) 48

4 DATA, DATA ANALYSIS AND INTERPRETATION 51
4.1 Data Analysis and Interpretation 51
4.2 Data 60
4.3 Dispersion 66
4.4 Error Analysis 67

5 SUMMARY AND CONCLUSIONS 70
5.1 Summary 70
5.2 Conclusions 71

Bibliography 72

List of Figures

1 *The shape of the orthorhombic mm2 crystal class.* 3

1.1 *Model to show anisotropic binding of an electron in a crystal.* 11
1.2 *The wave vector surface.* 15
1.3 *Intercept of the wave-vector surface in the xz plane for (a) biaxial crystals; (b) uniaxial positive crystal (c) uniaxial negative crystal.* 17
1.4 *Reflection and refraction of linearly polarized light at the interface between two optically different media.* 20
1.5 *Multiple reflection of light ray between two optically different media of refractive indices n_o and n_1.* 24

2.1 *The Jones vector of some state of polarization* 35
2.2 *$\vec{E}_i$ and $\vec{E}_o$ are the respective Jones vectors of plane waves incident on and emergent from the optical system S.* 36

3.1 *An optical diagram of a general ellipsometry arrangement for PSA.* . 50

4.1 *The transmission spectrum for KTP.* 53
4.2 *I-A curve for n_x at wavelength $\lambda = 632.8nm$.* 54
4.3 *I-A curve for n_y at wavelength $\lambda = 632.8nm$.* 55
4.4 *I-A curve for n_x at wavelength $\lambda = 804.4nm$.* 56
4.5 *I-A curve for n_y at wavelength $\lambda = 804.4nm$.* 57
4.6 *I-A curve for n_x at wavelength $\lambda = 808.4nm$.* 58
4.7 *I-A curve for n_y at wavelength $\lambda = 808.4nm$.* 59

4.8 *Dispersion graph of KTP crystal for n_x.* 66
4.9 *Dispersion graph of KTP crystal for n_y.* 67

Abstract

The Thesis discusses the use of reflection ellipsometry as a precise, and non-destructive technique for the determination of the optical constants of a Potassium Titanyl Phosphate (KTP) crystal. The KTP is a biaxial orthorhombic flux grown crystal. It has three refractive indices: n_x, n_y and n_z. Out of which only two linear refractive indices n_x and n_y for the two reflective faces correspond to x and y axis, respectively, could be measured while the third refractive index n_z could not be measured due to poor surface quality.

The refractive indices are measured at three wavelengths in its transmission range using He-Ne ($\lambda = 632.8nm$), and temperature tuned diode lasers ($\lambda = 804.4.nm$ and $\lambda = 808.4nm$). The obtained experimental data of the reflected intensity and analyzer angles are fitted to the theoretical model of curve fitting in the computer. The results of refractive indices are found in good agreement with the theoretical values. The relative errors are assessed up to $0.17\,o/o$ for the n_x at $\lambda = 632.8nm$ and $0.028\,o/o$ for n_y at $\lambda = 808.4nm$. We also demonstrate the normal behaviour of the experimental refractive indices n_x and n_y respectively.

Introduction

The optical effect that we experience every day are linear effects, or we can say that when light interacts with matter, the matter usually responds proportionately, and it is this proportionate response that leads to the familiar optical qualities of reflection, refraction, scattering and absorption.

These linear optical responses of matter modify light in many useful ways, but they do not alter the frequency of light. For example, after a beam of light from a typical laser source He-Ne laser passes through a lens, the wavelength is still $632.8nm$. The beam might not be headed in the same direction because of reflection, and it might not have the same intensity because of absorption and reflection, but at least it leaves the light with the same frequency. In 1961; however, Peter Franker and other at the university of Michigan witnessed an optical effect that was quite out of the ordinary effect. When they focused the high-power light from a ruby laser at a quartz crystal they found that the transmitted light consists of not one but two frequency components, with wavelength at $694.3nm$ and $347.15nm$. In stead of just transmitting the laser light, the crystal actually generated a second beam having exactly twice the frequency of the laser light. Though the intensity of the generated ultraviolet beam was very weak, but with in months, more harmonic optical effects were demonstrated and a new branch of optical science was born: "*Non Linear Optics*".

Nonlinear electromagnetic phenomena occur in materials when the response of the medium is a nonlinear function of the applied electric and magnetic field amplitudes.

The nonlinearities reside in the constitutive relationships of Maxwell's equations. The earliest nonlinear response were observed with the application of dc or low frequency electric and magnetic fields. A prime example is the magnetization curve of ferromagnetic materials, leading to hysteresis, remanence, and others. In 1875 [13] Kerr showed that the birefringence could be induced in optically isotropic media, such as glass and liquids, by the application of a dc electric field. He showed that the birefringence was proportional to the square of the dc field and observed that "the particles in the dielectrified bodies tend to arrange themselves in fields along the lines of force". The "changes in molecular rearrangements upon rise and fall of electric action are affected slowly in solids, and at once in liquids".

In materials optical nonlinearity occur when the response of the medium is a nonlinear function(s) (it can be second order or third order functions) of the applied electric field amplitude. In this thesis we have made an attempt to study the refractive index of KTP crystal an optically nonlinear material. Refractive index (R.I) is an optical property of a material. It is basically the ability of the material to slow down the speed of the propagation of a light wave as the light passes through it. R.1 is a wavelength dependent property.

The Crystal KTP

The solid material compound KTP was discovered and introduced in 1976 [14]. KTP belongs to the family of compounds that have the formula unit $MTiOXO_4$, where M can be K, Rb, Tl, NH_4, or Cs (partial) and X can be P or As. All members are ***orthorhombic*** and belong to the acentric point group $mm2$. For KTP, the lattice constants are $a = 12.814\dot{A}$, $b = 6.404\dot{A}$, and $c = 10.616\dot{A}$, and each unit cell contains eight formula units. The structure is characterized by chains of TiO_6 octahedra, which are linked at two corners, and the chains are separated by PO_4 tetrahedra (see fig. 1). [2, 7]

Large single crystals of KTP can be grown by two techniques: hydrothermal and

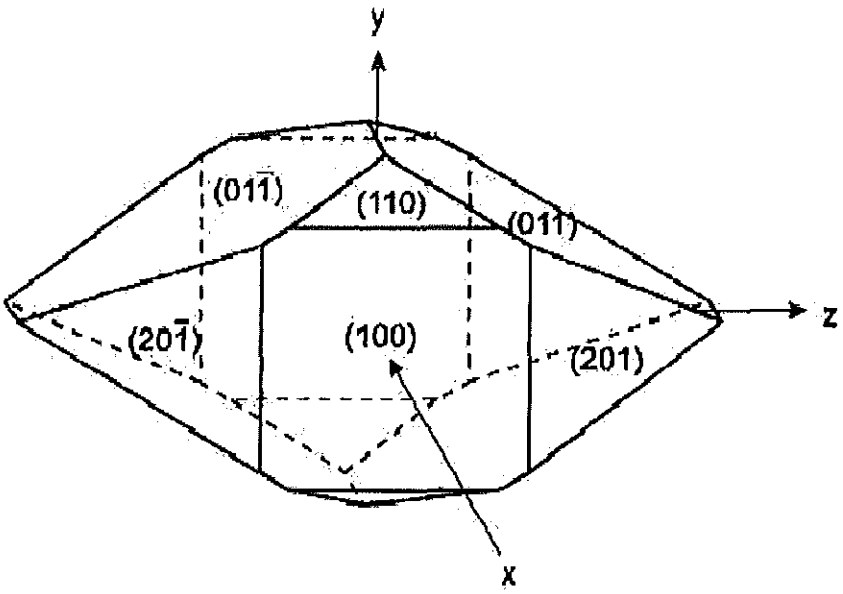

Figure 1: *The shape of the orthorhombic mm2 crystal class.*

flux techniques. Our KTP crystal is grown by flux growth technique. The flux technique is essentially a high temperature solution growth process in which the KTP crystallizes out of a molten KTP/flux composition when cooled. These morphologies (structures) of the crystal have their own optical qualities and properties which render KTP as a preferentially selected nonlinear material for different applications.

Potassium Titanyl Phosphate ($KTiOPO_4$; KTP) is a relatively new material [2] that has been shown to have superior properties for several nonlinear-optical applications and, in particular, for frequency doubling the $1064-\mu m$ radiation of Nd: YAG lasers. The KTP is also attractive for various sum-and difference-frequency and optical parametric applications over its entire transparency range from 0.35 to $4.5\mu m$. [3, 4, 5, 6]

Its high nonlinear optical d coefficients [2] made KTP to be widely used for frequency doubling Nd:YAG lasers and other Nd-doped laser systems. Its large nonlinear coefficients are phase matchable. This property, combined with low absorption and a wide acceptance angle makes it the preferred doubling crystal when the available pick power is limited. [7, 17] The unusually large temperature bandwidth of KTP is particularly advantageous for maintaining pulsed energy stability of the converted beam. [7, 8, 17] Its temperature bandwidth combined with relatively good thermal properties gives KTP an exceptionally good figure of merit for doubling high average-power-cw and quasi-cw beams. Recent experiments on intracavity frequency doubling have also shown that KTP is much less susceptible to bulk damage at relatively high average power-levels. In addition to having attractive nonlinear-optical characteristics, KTP has promising electro-optic and dielectric properties that make it potentially useful for various electro-optic applications. [2] KTP has an optical waveguide modulator figure of merit that is nearly $2\times$ greater than that for any other inorganic material. [2] Therefore, KTP, with its superior qualities described above, has attracted the writer's interest to study the optical constants of this material.

The method

In this thesis we are going to employ an *Ellipsometry* technique in order to find the optical constants of KTP crystal. Ellipsometry [1] is a technique of measurement of the state of polarization of a polarized light wave for the determination of optical constants such as R.I and thickness of semi-transparent thin films and dielectric crystals. Particularly we use a so called *Reflection Ellipsometry* technique. Reflection ellipsometry measures the changes in the state of polarization of light upon reflection from the surface of the material under investigation. In fact, there are different methods for the determination of R.I of a material. For a biaxial crystal a simple technique is minimum deviation method. But this technique works for materials cut

(grown) in the form of prism while our sample has orthorhombic shape. Transmission ellipsometry is another alternative method but this technique is useful when the optical system is transparent enough to make the transmitted wave accessible for measurement, and the optical sample is required to be plane-parallel section [18], which is not true for our sample. Other spectroscopic techniques require high-power light source which have their own disadvantage. So we employed reflection ellipsometry technique. As a non-invasive and non-destructive technique, ellipsometry requires only a low-power light source and, consequently, it does not affect most processes, which renders ellipsometry a convenient technique for *in situ* studies. [10]

The thesis contains five chapters. Chapter-1 deals with the interaction of light with matter. As we are dealing with the optical phenomena of light when it interacts with matter, therefore, it is important to discuss this aspect in detail. In addition, the Fresnel coefficients and Fabry-Perot equations are discussed to derive the general expression for the R.I of materials. The anisotropic and nonlinear aspects of biaxial crystals have also been discussed.

Chapter-2 deals with the concept of polarization, Jones vector and Jones matrix. The reflection ellipsometry is the core idea of Chapter-3. Chapter 4 contains the experimental data along with their analysiss, interpretation and discussion. Error analysis along with the results are also presented in this chapter. The final chapter, Chapter-5, summarizes the results and conclusions. Finally we would like to mention that this thesis presents the basic concepts and applications of ellipsometry technique for the determination of the optical constants of a biaxial KTP crystal in a simplified form, but the readers can find more details in the cited references.

Chapter 1

INTERACTION OF LIGHT WITH MATTER

1.1 Maxwell's Equations

A description of ellipsometry as an optical technique would not be complete without mentioning Maxwell's equations. Maxwell theory predicts that light is a wave represented by two mutually perpendicular vectors; the electric field $\vec{E}$ and the magnetic field $\vec{H}$. The electromagnetic state of a vacuum at a point is said to be specified by these two vectors, $\vec{E}$ and $\vec{H}$. In the static case, that is, when the two fields do not change with time, $\vec{E}$ and $\vec{H}$ are independent of one other and are determined, respectively, by the distribution of charges and currents in all space. Many of the optical properties of solids can be understood on the basis of classical electromagnetic theory. In the next section we apply the macroscopic Maxwell theory to the propagation of light through dielectric medium. The electromagnetic state of matter at a given point is described by four quantities: (1) the volume density of electric charge ρ, (2) the volume density of magnetic dipoles, called the *polarization* $\vec{P}$, (3) the volume density of magnetic dipoles, called the *magnetization* $\vec{M}$ and (4) the electric current per unit area, called the *current density* $\vec{J}$. We shall be concerned only with nonmagnetic, electrically neutral medium ($\vec{M}$ and ρ are zero). For such case Maxwell's Equations

take the form

$$\vec{\nabla} \times \vec{E} = -\mu_o \frac{\partial \vec{H}}{\partial t} \tag{1.1.1}$$

$$\vec{\nabla} \times \vec{H} = \epsilon_o \frac{\partial \vec{E}}{\partial t} + \frac{\partial \vec{P}}{\partial t} + \vec{J} \tag{1.1.2}$$

$$\vec{\nabla} \cdot \vec{E} = -\frac{1}{\epsilon_o} \vec{\nabla} \cdot \vec{P} \tag{1.1.3}$$

$$\vec{\nabla} \cdot \vec{H} = 0 \tag{1.1.4}$$

The general wave equation for the $\vec{E}$ filed is obtained by taking the curl of Eq. (1.1.1) and the time derivative of Eq. (1.1.2)and eliminating $\vec{H}$. The result is

$$\vec{\nabla} \times (\vec{\nabla} \times \vec{E}) + \frac{1}{c^2} \frac{\partial^2 \vec{E}}{\partial t^2} = -\mu_o \frac{\partial^2 \vec{P}}{\partial t^2} - \mu_o \frac{\partial \vec{J}}{\partial t}. \tag{1.1.5}$$

1.2 Propagation of Light in Dielectric Materials

In order to understand the propagation of light through dielectric materials, we take the case of a nonconducting and isotropic medium. For a simple isotropic dielectric material the electrons are permanently bound to the atoms comprising the medium and there is no preferential direction. Suppose that each electron, of charge $-e$, in a dielectric is displaced a distance $\vec{r}$ from its equilibrium position. The resulting macroscopic polarization $\vec{P}$ of the medium is given by

$$\vec{P} = -Ne\vec{r} \tag{1.2.1}$$

where N is the number of electron per unit volume. If the displacement of the electron is the result of the application of the static electric field $\vec{E}$, and if the electron is elastically bound to its equilibrium position with a force constant K, then the force equation is

$$-e\vec{E} = K\vec{r}. \tag{1.2.2}$$

Here we can assume two cases:The first is the static polarization, where the polarization is given, from Eqs. (1.2.1) and (1.2.2), by

$$\vec{P} = \frac{Ne^2}{K}\vec{E}. \tag{1.2.3}$$

However, in order to find the true polarization we take the field $\vec{E}$ to vary with time and we must take the actual motion of the electron into account. To do this we consider the bound electrons as classical damped harmonic oscillators. The differential equation of motion is

$$m\frac{d^2\vec{r}}{dt^2} + m\gamma\frac{d\vec{r}}{dt} + K\vec{r} = -e\vec{E}. \tag{1.2.4}$$

The term $m\gamma(\frac{d\vec{r}}{dt})$ represents a frictional damping force that is proportional to the velocity of the electron, the proportional constant being written as $m\gamma$. Now suppose that the applied electric field varies harmonically with time according to the usual factor $e^{-i\omega t}$. Assuming that the motion of the electron has the same harmonic time dependence, we find that Eq. (1.2.4) becomes

$$(-m\omega^2 - i\omega m\gamma + K)\vec{r} = -e\vec{E}. \tag{1.2.5}$$

Consequently, the polarization, from Eq. (1.2.1), is given by

$$\vec{P} = \frac{Ne^2}{-m\omega^2 - i\omega m\gamma + K}\vec{E}. \tag{1.2.6}$$

This equation reduces to the static value, Eq. (1.2.3), when $\omega = 0$. Thus for a given amplitude of the impressed electric field, the amount of polarization varies with frequency. The phase of $\vec{P}$, relative to that of the electric field, also depends on the frequency. This is shown by the presence of the imaginary term in the denominator. A more significant way of writing Eq. (1.2.6) is

$$\vec{P} = \frac{Ne^2/m}{\omega_o^2 - \omega^2 - i\omega\gamma}\vec{E} \tag{1.2.7}$$

in which we have introduced the abbreviation ω_o given by $\omega_o = \sqrt{\frac{K}{m}}$. The polarization formula Eq. (1.2.7) is similar to the amplitude formula for a driven harmonic

oscillator, as indeed it should be, since it is the displacement of the elastically bound electrons that actually constitutes the polarization. We should therefore expect to find an optical resonance phenomenon of some kind occurring for light frequencies in the neighborhood of the resonance frequency ω_o. This resonance phenomenon is manifested as a large change in the R.I of the medium and also by a strong absorption of light at or near the resonance frequency [11]. Now to see how the polarization affects the propagation of light, let us see the general wave equation. For a dielectric there is no conduction term. Hence we have

$$\vec{\nabla} \times (\vec{\nabla} \times \vec{E}) + \frac{1}{c^2}\frac{\partial^2 \vec{E}}{\partial t^2} = \frac{-\mu_o N e^2}{m}\left(\frac{1}{\omega_o^2 - \omega^2 - i\gamma\omega}\right)\frac{\partial^2 \vec{E}}{\partial t^2}. \tag{1.2.8}$$

Also, from the linear relationship between $\vec{P}$ and $\vec{E}$, it follows from Eq. (1.1.3) that $\vec{\nabla} \cdot \vec{E} = 0$. Consequently, $\vec{\nabla} \times (\vec{\nabla} \times \vec{E}) = -\nabla^2 \vec{E}$, and Eq. (1.2.8) reduces to

$$\nabla^2 \vec{E} = \frac{1}{c^2}\left(1 + \frac{Ne^2}{m\epsilon_o}.\frac{1}{\omega_o^2 - \omega^2 - i\gamma\omega}\right)\frac{\partial^2 \vec{E}}{\partial t^2} \tag{1.2.9}$$

where we used $\frac{1}{c^2} = \mu_o \epsilon_o$. Let us seek a solution of the form

$$\vec{E} = \vec{E}_o e^{i(\mathrm{K}z - \omega t)}. \tag{1.2.10}$$

This trial solution represents what are called homogeneous plane harmonic waves. Direct substitution shows that this is a possible solution provided that

$$\mathrm{K}^2 = \frac{\omega^2}{c^2}\left(1 + \frac{Ne^2}{m\epsilon_o}.\frac{1}{\omega_o^2 - \omega^2 - i\gamma\omega}\right). \tag{1.2.11}$$

The presence of the imaginary term in the denominator implies that the wavenumber K must be a complex number [11]. Thus, we can express K in terms of its real and imaginary parts as

$$\mathrm{K} = k + i\alpha \tag{1.2.12}$$

This amounts to the same thing as introducing a complex index of refraction

$$n = n_o + i\kappa \tag{1.2.13}$$

where

$$\mathrm{K} = \frac{\omega}{c} n. \tag{1.2.14}$$

Our solution in Eq. (1.2.10) can then be written as

$$\vec{E} = \vec{E}_o e^{-\alpha z} e^{i(kz-\omega t)}. \tag{1.2.15}$$

The factors $e^{\alpha z}$ indicates that the amplitude of the wave decreases exponentially with distance. This means that as the wave propagates, the energy of the wave is absorbed by the medium. Since the energy in the wave at a given point is proportional to $|\vec{E}|^2$, then the energy varies with distance as $e^{-2\alpha z}$. Hence 2α is the *coefficient of absorption* of the medium. The imaginary part κ of the complex R.I is known as the *extinction index*. The two numbers α and κ are related by the equation

$$\alpha = \frac{\omega}{c} \kappa \tag{1.2.16}$$

or

$$a = \frac{4\pi}{\lambda} \kappa \tag{1.2.17}$$

where $a = 2\alpha$ is the absorption coefficient of the medium. Hence, from Eqs. (1.2.16) and (1.2.17) one can understand that for a medium to have imaginary part in its R.I, its absorption coefficient must not be vanish.

1.3 Propagation of Light in a Crystal

The distinguishing basic feature of the crystalline state, as far as optical properties are concerned, is the fact that most crystals are electrically anisotropic. This means that the polarization produced in the crystal by a given electric field is not just a simple scalar constant times the electric field, but varies in a manner that depends on the direction of the applied field in relation to the crystal lattice. One of the consequences is that the speed of a propagation of a light wave in a crystal is a function of the

direction of propagation and the polarization of the light [11].

There are two values of the phase velocity for a given direction of propagation. These two values are associated with two mutually orthogonal polarization of the light waves. Crystals are said to be *doubly refracting* or *birefringent.* [11] A model to illustrate the anisotropic polarizability of a crystal is shown in figure 1.1. A bound electron is

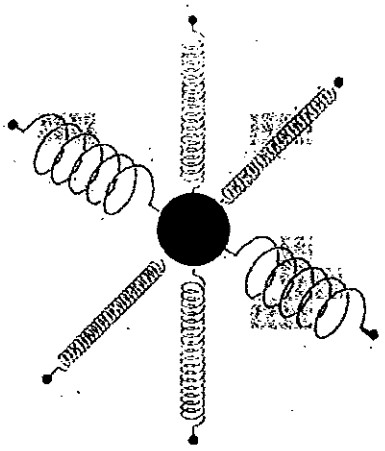

Figure 1.1: *Model to show anisotropic binding of an electron in a crystal.*

pictured here as attached a set of fictitious elastic springs. The sprigs have different stiffnesses for different directions of the electron displacement from its equilibrium position within the crystal lattice. The displacement of the electron under the action of the external field $\vec{E}$ depends on the direction of the field as well as its magnitude. This is also true for the resulting polarization $\vec{P}$. The displacement of $\vec{P}$ on $\vec{E}$ is expressible as a tensor relation in the form

$$\begin{pmatrix} P_x \\ P_y \\ P_z \end{pmatrix} = \epsilon_o \begin{pmatrix} \chi_{11} & \chi_{12} & \chi_{13} \\ \chi_{21} & \chi_{22} & \chi_{23} \\ \chi_{31} & \chi_{32} & \chi_{33} \end{pmatrix} \begin{pmatrix} E_x \\ E_y \\ E_z \end{pmatrix}. \tag{1.3.1}$$

This is customarily written as

$$\vec{P} = \epsilon_o \chi \vec{E} \tag{1.3.2}$$

where χ is the susceptibility tensor:

$$\chi = \begin{pmatrix} \chi_{11} & \chi_{12} & \chi_{13} \\ \chi_{21} & \chi_{22} & \chi_{23} \\ \chi_{31} & \chi_{32} & \chi_{33} \end{pmatrix}. \tag{1.3.3}$$

The corresponding displacement vector $\vec{D}$ is given by $\vec{D} = \epsilon_o(1+\chi)\vec{E} = \epsilon\vec{E}$, where $\mathbf{1}$ is a unit matrix

$$\mathbf{1} = \begin{pmatrix} 1 & 0 & 0 \\ 0 & 1 & 0 \\ 0 & 0 & 1 \end{pmatrix}$$

and

$$\epsilon = \epsilon_o(1+\chi),$$

which is the dielectric tensor.

For the ordinary non absorbing crystal χ-tensor is symmetric [11] so there always exists a set of coordinate axes, called principal axes, such that the χ tensor assumes the diagonal form

$$\chi = \begin{pmatrix} \chi_{11} & 0 & 0 \\ 0 & \chi_{22} & 0 \\ 0 & 0 & \chi_{33} \end{pmatrix}. \tag{1.3.4}$$

The three χs are known as the principal susceptibilities. Corresponding to these, the quantities $K_{11} = 1+\chi_{11}$, ... and so forth, are called the principal *dielectric constants.* In view of Eq. (1.3.2), the general wave equation Eq. (1.1.5) can be written as

$$\vec{\nabla} \times (\vec{\nabla} \times \vec{E}) + \frac{1}{c^2}\frac{\partial^2 \vec{E}}{\partial t^2} = -\frac{1}{c^2}\chi\frac{\partial^2 \vec{E}}{\partial t^2}. \tag{1.3.5}$$

For a monochromatic plane wave of the form $e^{i(\vec{k}.\vec{r}-\omega t)}$, Eq. (1.3.5) is similar to

$$\vec{k} \times (\vec{k} \times \vec{E}) + \frac{\omega^2 \vec{E}}{c^2} = -\frac{\omega^2}{c^2}\chi\vec{E}. \tag{1.3.6}$$

In terms of components the above Eq. (1.3.6) is equivalently written into three equations:

$$(-k_y^2 - k_z^2 + \frac{\omega^2}{c^2})E_x + k_x k_y E_y + k_x k_z E_z = -\frac{\omega^2}{c^2}\chi_{11}E_x \tag{1.3.7}$$

$$k_y k_x E_x + (-k_x^2 - k_z^2 + \frac{\omega^2}{c^2})E_y + k_y k_z E_z = -\frac{\omega^2}{c^2}\chi_{22}E_y \tag{1.3.8}$$

$$k_z k_x E_x + k_z k_y E_y + (-k_x^2 - k_y^2 + \frac{\omega^2}{c^2})E_z = -\frac{\omega^2}{c^2}\chi_{33}E_z. \tag{1.3.9}$$

In order to interpret the physical meaning of these equations, suppose we have a particular case of a wave propagating in the direction of one of the principal axes, say the x axis. In this case $k_x = k$, $k_y = k_z = 0$, and the three equations reduce to

$$\begin{aligned} \tfrac{\omega^2}{c^2}E_x &= -\tfrac{\omega^2}{c^2}\chi_{11}E_x \\ (-k^2 + \tfrac{\omega^2}{c^2})E_y &= -\tfrac{\omega^2}{c^2}\chi_{22}E_y \\ (-k^2 + \tfrac{\omega^2}{c^2})E_z &= -\tfrac{\omega^2}{c^2}\chi_{33}E_z \end{aligned} \tag{1.3.10}$$

The first equation implies that $E_x = 0$, because neither ω nor χ_{11} is zero. This means that the $\vec{E}$ filed is transverse to the x axis, which is the direction of propagation. Consider next the second equation. If $E_y \neq 0$, then

$$k = \frac{\omega}{c}\sqrt{1+\chi_{22}} = \frac{\omega}{c}\sqrt{K_{22}}. \tag{1.3.11}$$

The third equation, likewise implies that if $E_z \neq 0$, then

$$k = \frac{\omega}{c}\sqrt{1+\chi_{33}} = \frac{\omega}{c}\sqrt{K_{33}}. \tag{1.3.12}$$

Now ω/k is the phase velocity of the wave. Thus we have two possible phase velocities, namely, $c/\sqrt{K_{22}}$ if the $\vec{E}$ vector points in the y direction, and $c/\sqrt{K_{33}}$ if the $\vec{E}$ vector points in the z direction.

More generally we can show that for any direction of the propagation vector $\vec{k}$, there are two possible values of the magnitude k and hence two values of the phase velocity.

To do this, let us introduce the three *principal indices of refraction* n_1, n_2 and n_3 defined by

$$\begin{aligned} n_1 &= \sqrt{1+\chi_{11}} = \sqrt{K_{11}} \\ n_2 &= \sqrt{1+\chi_{22}} = \sqrt{K_{22}} \\ n_3 &= \sqrt{1+\chi_{33}} = \sqrt{K_{33}} \end{aligned} \tag{1.3.13}$$

Now in Eqs. (1.3.7) to (1.3.9), in order for a nontrivial solution for E_x, E_y and E_z to exist, the determinant of the coefficients must vanish; i.e.,

$$\begin{vmatrix} (n_1\omega/c)^2 - k_y^2 - k_z^2 & k_xk_y & k_xk_z \\ k_yk_x & (n_2\omega/c)^2 - k_x^2 - k_z^2 & k_yk_z \\ k_zk_x & k_zk_y & (n_3\omega/c)^2 - k_x^2 - k_y^2 \end{vmatrix} = 0 \tag{1.3.14}$$

where we have used Eq. (1.3.13). The above equation can be represented by a three dimensional surface in $\vec{k}$ space. The form of this $\vec{k}$ surfaces, or wave vector-surfaces is shown in figure 1.2. To see how the surface is constructed, consider any one of the coordinate planes, say the xy plane. In this plane $k_z = 0$, and the determinant reduces to the product of the two factors

$$[(\frac{n_3\omega}{c})^2 - k_x^2 - k_y^2]\{[(\frac{n_1\omega}{c})^2 - k_y^2][(\frac{n_2\omega}{c})^2 - k_x^2] - k_x^2k_y^2\} = 0. \tag{1.3.15}$$

Since the product must vanish, either or both of the factors must be equal to zero. Setting the first factor equal to zero gives the equation of a circle

$$k_x^2 + k_y^2 = (\frac{n_3\omega}{c})^2 \tag{1.3.16}$$

The second factor gives the equation of an ellipse

$$\frac{k_x^2}{(n_2\omega/c)^2} + \frac{k_y^2}{(n_1\omega/c)^2} = 1. \tag{1.3.17}$$

Similar equations are obtained for the xz and yz planes. The intercept of $\vec{k}$ surface with each coordinate plane therefore consists of one circle and one ellipse as shown. The complete $\vec{k}$ surface is double; that is, it consists of an inner sheet and an outer

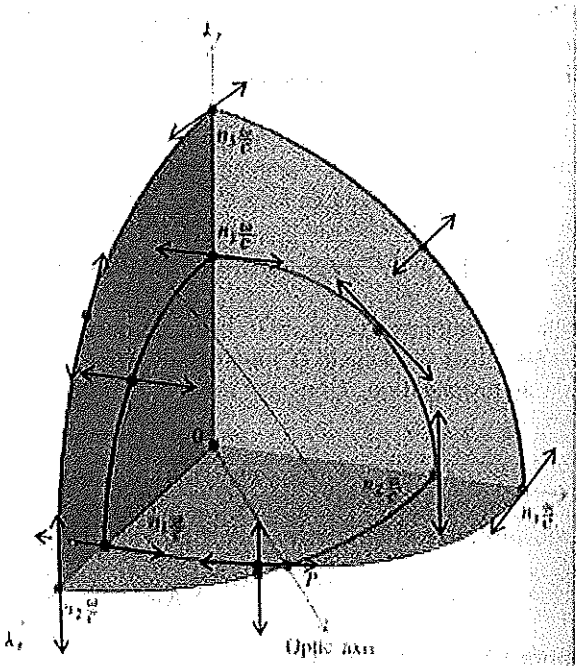

Figure 1.2: *The wave vector surface.*

sheet. This implies that for any given direction of the wave vector $\vec{k}$, there are two values for the wavenumber k. It follows that there are also two values of the phase velocity. Now we just showed that for a wave propagating in the x direction, the two phase velocities corresponding to two mutually orthogonal directions of polarization. It turns out that the same is true for any direction of propagation; that is, the two phase velocities correspond to two mutually orthogonal polarizations. Now, as we know, a light wave of arbitrary polarization can always be resolved into two orthogonally polarized waves. Hence, when unpolarized light, or light of arbitrary polarization propagates through a crystal, it can be considered to consists of two independent waves that are polarized orthogonally with respect to each other and travelling with different phase velocities.

The nature of the $\vec{k}$ surface is such that the inner and outer sheets touch at a certain

point P as shown in figure 1.2. This point defines a direction for which the two values of k are equal. The direction so defined is called an *optic axis* of the crystal. [11] Thus, when propagating in the direction of an optic axis, the phase velocities of the two orthogonally polarized waves reduce to the same value.

The general case is shown in figures 1.2 and 1.3*a*. Here the three principal indices n_1, n_2 and n_3 are all different. We can see from the intercepts that there are *two* optic axes. In this case the crystal is said to be *biaxial.* If two of the principal indices are equal, in which case there is only *one* optic axis and the crystal is called *uniaxial.* The $\vec{k}$ surface for a uniaxial crystal consists of a sphere and an ellipsoid of revolution, the axis of which is the optic axis of the crystal (figure 1.3*b* and *c*). If all the three indices are equal, then the $\vec{k}$ surface degenerates to a single sphere, and the crystal is not doubly refracting at all but is optically isotropic.

In view of the fact that the principal indices are related to the components of the χ tensor by Eq. (1.3.13), we can conveniently classify crystals according to the χ tensor as follows:

$$
\begin{array}{lll}
Isotropic & \chi = \begin{pmatrix} a & 0 & 0 \\ 0 & a & 0 \\ 0 & 0 & a \end{pmatrix} & \chi_{11} = \chi_{22} = \chi_{33} = a \\
 & & n = \sqrt{1+a} \\
Uniaxial & \chi = \begin{pmatrix} a & 0 & 0 \\ 0 & a & 0 \\ 0 & 0 & b \end{pmatrix} & \chi_{11} = \chi_{22} = a, \chi_{33} = b \\
 & & n_o = \sqrt{1+a} \\
 & & n_E = \sqrt{1+b} \\
Biaxial & \chi = \begin{pmatrix} a & 0 & 0 \\ 0 & b & 0 \\ 0 & 0 & c \end{pmatrix} & \chi_{11} = a, \chi_{22} = b, \chi_{33} = c \\
 & & n_1 = \sqrt{1+a} \\
 & & n_2 = \sqrt{1+b} \\
 & & n_3 = \sqrt{1+c}
\end{array}
\qquad . \qquad (1.3.18)
$$

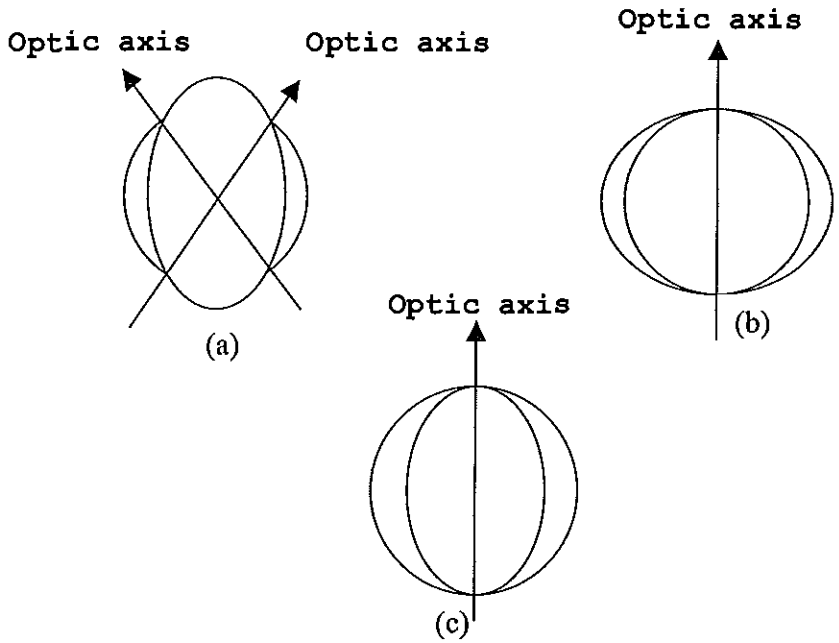

Figure 1.3: *Intercept of the wave-vector surface in the xz plane for (a) biaxial crystals; (b) uniaxial positive crystal (c) uniaxial negative crystal.*

1.4 Propagation of Light Across a Plane Interface of Nonconducting (Dielectric) Materials

We consider a more general case that an electromagnetic (em) wave of frequency ω and amplitude E_1 incident on the plane interface of two simple (linear) materials of R.Is n_o and n_1. Figure 1.4 shows that how a beam of linearly polarized light incident(i) on a bare surface is reflected(r) at the interface between two optically differeut media. The plane of incidence (POI) includes the incident beam and the sample surface normal $\hat{n}$, which is the plane of the paper. The components parallel (E_p) and perpendicular (E_s) to the POI are out of phase after reflection, and both phase and

amplitude of the reflected light change in a distinct way depending on the optical properties of the surface. It is assumed that the change in the R.I is abrupt (a step function) across the interface.

The wave incident from medium 0 gives rise to a reflected wave in the same medium and a transmitted wave in medium 1. The angle of incidence θ_0 and the angle of reflection θ_1 are both measured from the direction of the normal to the interface. The total fields inside media 0 and 1 obeys Maxwell's equations and the boundary conditions at the interface. For a given amplitude and polarization of the incident wave, the amplitude and polarization of the reflected and transmitted waves can be determined from the continuity of the tangential components of the $\vec{E}$ and $\vec{H}$ field vectors across the interface. When the incident wave is linearly polarized with the electric vector vibrating parallel (p) to the plane of incidence, the reflected and transmitted waves are similarly polarized with their electric vectors also vibrating parallel to the plane of incidence. Likewise, when the incident wave is linearly polarized perpendicular (s) to the plane of incidence, the reflected and transmitted waves are also linearly polarized to the same plane. In other words, the eigenpolarizations of reflection and transmission are the linear vibrations parallel (p) and perpendicular (s) to the plane of incidence.[1]

1.4.1 Fresnel Coefficients

It is adequate to determine the (electric field) amplitudes of the reflected and transmitted waves in terms of those of the incident wave for the p and s polarizations only. This is because an arbitrarily polarized incident wave can be resolved into its p and s components, each then is treated separately and the results are latter combined. The reason why we chose electric field in our treatment will be apparent in Chapter 2.

P-Polarization

This is the case when the component of the wave (electric field)is polarized in the plane of incidence. The reflected and transmitted waves are taken to propagate in the plane of incidence which is in the plane of $\vec{k_o}$ and the normal to the interface (plane of the page). We take the frequencies of the three waves to be identical. Thus for the electric and magnetic fields we write

Incident wave:

$$\vec{E_i} = \vec{E_o} \exp(i[\vec{k_o}.\vec{r} - \omega t]) \tag{1.4.1}$$

$$\vec{H_i} = \frac{n_o}{c}\vec{k_o} \times \vec{E_o} \exp(i[\vec{k_o}.\vec{r} - \omega t]) \tag{1.4.2}$$

Reflected wave:

$$\vec{E_r} = \vec{E_o'} \exp(i[\vec{k_o'}.\vec{r} - \omega t]) \tag{1.4.3}$$

$$\vec{H_r} = \frac{n_o}{c}\vec{k_o'} \times \vec{E_o'} \exp(i[\vec{k_o'}.\vec{r} - \omega t]) \tag{1.4.4}$$

Transmitted wave:

$$\vec{E_t} = \vec{E_1} \exp(i[\vec{k_1}.\vec{r} - \omega t]) \tag{1.4.5}$$

$$\vec{H_t} = \frac{n_1}{c}\vec{k_1} \times \vec{E_1} \exp(i[\vec{k_1}.\vec{r} - \omega t]), \tag{1.4.6}$$

where $\vec{k_o}, \vec{k_o'}$ and $\vec{k_1}$ are the propagation vectors of the wave. We apply boundary conditions; i.e., at the interface $z = 0$ the tangential components of the electric and magnetic fields are continuous; i.e.,

$$E_o \cos\theta_o \exp(i[\vec{k_o}.\vec{\rho}]) - E_o' \cos\theta_o' \exp(i[\vec{k_o'}.\vec{\rho}]) = E_1 \cos\theta_1 \exp(i[\vec{k_1}.\vec{\rho}]) \tag{1.4.7}$$

and

$$n_o E_o \exp(i[\vec{k_o}.\vec{\rho}]) + n_o E_o' \exp(i[\vec{k_o'}.\vec{\rho}]) = n_1 E_1 \exp(i[\vec{k_1}.\vec{\rho}]). \tag{1.4.8}$$

For this two conditions to be satisfied at any point on the interface, the phase factors have to be first matched and then the amplitudes have to be related appropriately.

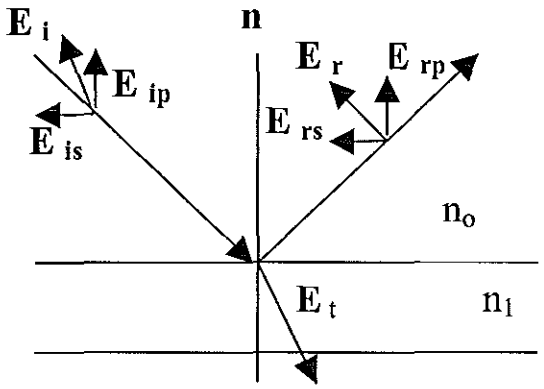

Figure 1.4: *Reflection and refraction of linearly polarized light at the interface between two optically different media.*

Thus phase matching requires

$$\vec{k_o}.\vec{\rho} = \vec{k_o'}.\vec{\rho} = \vec{k_1}.\vec{\rho}, \tag{1.4.9}$$

and amplitudes are related as

$$E_o \cos\theta_o - E_o' \cos\theta_o' = E_1 \cos\theta_1 \tag{1.4.10}$$

and

$$n_o(E_o + E_o') = n_1 E_1. \tag{1.4.11}$$

Since $\vec{\rho} = -\hat{n} \times (\hat{n} \times \vec{\rho})$ where $\hat{n}$ is a unit vector normal to the interface and away from material 1, then

$$(\vec{k}.\vec{\rho}) = -(\vec{k} \times \hat{n}).(\hat{n} \times \vec{\rho}). \tag{1.4.12}$$

Hence using Eq. (1.4.12) into Eq. (1.4.9) confirms that $\vec{k_o}, \vec{k_o'}$ and $\vec{k_1}$ are coplanar with magnitude relation given by

$$k_o \sin\theta_o = k_o' \sin\theta_o' = k_1 \sin\theta_1 \tag{1.4.13}$$

which leads to

$$\theta_o = \theta_o', \tag{1.4.14}$$

which is called the law of reflection. Again from Eq. (1.4.13) we get $k_o \sin\theta_o = k_1 \sin\theta_1$, which leads to

$$n_o \sin\theta_o = n_1 \sin\theta_1, \tag{1.4.15}$$

which is called the law of refraction (Snell's law). If media 0 and 1 are transparents, so that n_o and n_1 are both real numbers, the angles θ_o and θ_1 are also real. However, when either one or both media are absorbing, the angles θ_o and θ_1 become, in general, complex. [1] The reflection and transmission coefficients, also called *Fresnel coefficients*, are determined as

$$r_{o1p} = \frac{E_o'}{E_o} \tag{1.4.16}$$

and

$$t_{o1p} = \frac{E_1}{E_o} \tag{1.4.17}$$

Using Eqs. (1.4.10) and (1.4.11) the value of E_o' and E_1 are given as

$$E_o' = \frac{n_1\cos\theta_o - n_o\cos\theta_1}{n_1\cos\theta_o + n_o\cos\theta_1} E_o \tag{1.4.18}$$

and

$$E_1 = \frac{2n_o\cos\theta_o}{n_1\cos\theta_o + n_o\cos\theta_1} E_o, \tag{1.4.19}$$

respectively. Then the reflection and transmission Fresnel coefficients, Eqs. (1.4.16) and (1.4.17) become

$$r_{o1p} = \frac{n_1\cos\theta_o - n_o\cos\theta_1}{n_1\cos\theta_o + n_o\cos\theta_1} \tag{1.4.20}$$

and

$$t_{o1p} = \frac{2n_o\cos\theta_o}{n_1\cos\theta_o + n_o\cos\theta_1}, \tag{1.4.21}$$

respectively.

S-Polarization

In this case the electric field of the incident wave is normal to the plane of incidence, and therefore the magnetic field lies in the plane of incidence. In this case the polarization of the magnetic field changes up on reflection and transmission instead of that of the electric field. The continuity of the tangential components of the $\vec{E}$ and $\vec{H}$ fields are given by

$$\vec{E_o}\exp(i[\vec{k_o}.\vec{\rho}]) + \vec{E_o'}\exp(i[\vec{k_o'}.\vec{\rho}]) = \vec{E_1}\exp(i[\vec{k_1}.\vec{\rho}]) \tag{1.4.22}$$

and

$$n_o E_o \cos\theta_o \exp(i[\vec{k_o}.\rho]) - n_o E_o' \cos\theta_o' \exp(i[\vec{k_o'}.\rho]) = n_1 E_1 \cos\theta_1 \exp(i[\vec{k_1}.\rho]). \tag{1.4.23}$$

Phase matching reduces the above equations to

$$E_o + E_o' = E_1 \tag{1.4.24}$$

$$n_o E_o \cos\theta_o - n_o E_o' \cos\theta_o = n_1 E_1 \cos\theta_1. \tag{1.4.25}$$

The Fresnel reflection and transmission coefficients are then

$$r_{o1s} = \frac{E_o'}{E_o} = \frac{n_o\cos\theta_o - n_1\cos\theta_1}{n_o\cos\theta_o + n_1\cos\theta_1} \tag{1.4.26}$$

and

$$t_{o1s} = \frac{E_1}{E_o} = \frac{2n_o\cos\theta_o}{n_o\cos\theta_o + n_1\cos\theta_1} \tag{1.4.27}$$

respectively.

Generally, the Fresnel coefficients, dropping the subscripts 0 and 1, are collected as

$$r_p = \frac{n_1\cos\theta_o - n_o\cos\theta_1}{n_1\cos\theta_o + n_o\cos\theta_1}, \tag{1.4.28}$$

$$t_p = \frac{2n_o\cos\theta_o}{n_1\cos\theta_o + n_o\cos\theta_1}, \tag{1.4.29}$$

$$r_s = \frac{n_o \cos\theta_o - n_1 \cos\theta_1}{n_o \cos\theta_o + n_1 \cos\theta_1} \tag{1.4.30}$$

and

$$t_s = \frac{2n_o \cos\theta_o}{n_o \cos\theta_o + n_1 \cos\theta_1} \tag{1.4.31}$$

with

$$n_o \sin\theta_o = n_1 \sin\theta_1. \tag{1.4.32}$$

If the electric field is parallel to the plane of incidence, the reflectivity R_p is given by

$$R_p = r_p . r_p^* \tag{1.4.33}$$

and if the electric field is perpendicular to the plane of incidence, the reflectivity $R_s$is given by

$$R_s = r_s . r_s^* \tag{1.4.34}$$

where r_p^* and r_s^* are the respective complex conjugate of the reflection coefficients r_p and r_s. The reflection coefficients in Eqs. (1.4.20) and (1.4.26) can also be obtained by using Fabry-Perot equations,which will be discussed in the next section.

1.4.2 Fabry-Perot Equations

Consider the light wave that interacts with the sample of R.I n_1 as shown in figure 1.5. Suppose the amplitude of the incident wave is A_o. At the first interface part of the light will be reflected and part of the light will be transmitted through the front surface of the sample. Further this transmitted light will get partly reflected from and transmitted through the back interface. This reflected light from the back interface will continue to be reflected and transmitted when it reaches at the two interfaces. Of course, the amplitudes (and also the intensity) of the light reflected and transmitted from the sample material get decreased. Then the amplitude A_r of the reflected light from the sample is the total sum of the amplitude of each reflected light ray; i.e.,

$$A_r = A_1 + A_2 + A_3 + ... \tag{1.4.35}$$

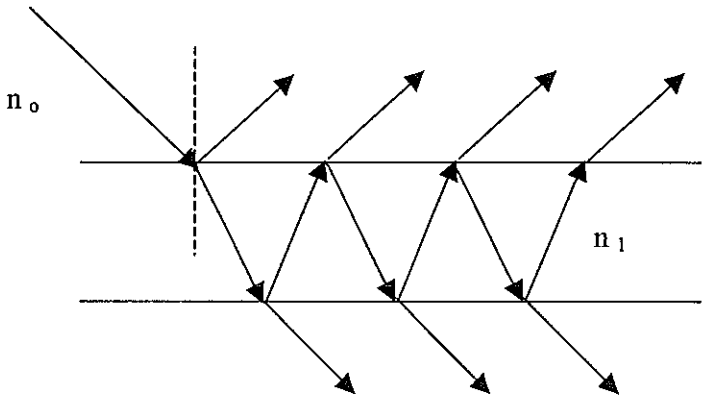

Figure 1.5: *Multiple reflection of light ray between two optically different media of refractive indices n_o and n_1.*

Or

$$A_r = A_o r = A_o r_{o1} + A_o t_{o1} r_{1o} t_{1o} e^{-i\delta} + A_o t_{o1} t_{1o} r_{1o}^3 e^{-i2\delta} + A_o t_{o1} t_{1o} r_{1o}^5 e^{-i3\delta} + ... \tag{1.4.36}$$

where δ is the phase difference between the reflected and the incident light, r is the total reflection coefficient; r_{o1} and r_{1o} are the respective reflection coefficients from the first to the second medium and the reverse, and t_{o1} and t_{1o} are the respective transmission coefficients from the first to the second medium and the reverse. then the ratio of the amplitudes of the reflected to the incident light A_r (which is the reflection coefficient) is given by

$$r = \frac{A_r}{A_o} = r_{o1} + t_{o1} r_{1o} t_{1o} \exp(-i\delta) + t_{o1} t_{1o} r_{1o}^3 \exp(-i2\delta) + t_{o1} t_{1o} r_{1o}^5 \exp(-i3\delta) + ... \tag{1.4.37}$$

Using the relation

$$t_{o1} + r_{o1} = 1 \tag{1.4.38}$$

$$t_{1o} + r_{1o} = 1 \tag{1.4.39}$$

and

$$r_{1o} = -r_{o1}, \tag{1.4.40}$$

we can write Eq. (1.4.37) as

$$r = r_{o1} + (1 - r_{o1})(1 - r_{1o})r_{1o}e^{-i\delta} + (1 - r_{o1})(1 - r_{1o})r_{1o}^3e^{-2i\delta} + (1 - r_{o1})(1 - r_{1o})r_{1o}^5e^{-3i\delta} + ... \tag{1.4.41}$$

Using summation rule for geometric progress, one can write Eq. (1.4.41) as

$$\hat{r} = \frac{r_{o1} - r_{o1}e^{-i\delta}}{1 - r_{o1}^2e^{-i\delta}}. \tag{1.4.42}$$

Eq. (1.4.42) is the reflection coefficient and also called *Fabry-Perot equation* with phase shift δ given by

$$\delta = \frac{4\pi d \cos\theta_1}{\lambda} \tag{1.4.43}$$

where d is the thickness, n_1 is the refractive index of the sample and λ is the wavelength of the incident light. The hat notation in r indicates that it is a phaser.

For the two mode of polarization, p or s polarization, we can write Eq. (1.4.42), the Fabry-Perot equation, as

$$\hat{r}_p = r_{TM} = \frac{A_{rp}}{A_{op}} = \frac{r_{o1p} - r_{o1p}e^{-i\delta}}{1 - r_{o1p}^2e^{-i\delta}} \tag{1.4.44}$$

and

$$\hat{r}_s = r_{TE} = \frac{A_{rs}}{A_{os}} = \frac{r_{o1s} - r_{o1s}e^{-i\delta}}{1 - r_{o1s}^2e^{-i\delta}} \tag{1.4.45}$$

The ratio of the two reflection coefficients can be splitted into an amplitude and phase factor, there by defining the ellipsometer angles Ψ and Δ as[8]

$$\hat{\rho} = \frac{r_p}{r_s} = \frac{r_{TM}}{r_{TE}} = \tan\Psi e^{i\Delta}. \tag{1.4.46}$$

The ellipsometer angles Ψ and Δ determine the differential changes in amplitude and phase, respectively, experienced upon reflection by the components vibrations of the electric vector parallel and perpendicular to the plane of incidence. The next step is to determine the values of the ellipsometer parameters Ψ and Δ there by ρ from the ellipsometry technique, which we shall discuss it in detail in Chapter-3.

Chapter 2

THE POLARIZATION OF LIGHT WAVES

Polarization is a property that is common to all types of vector waves. Electromagnetic waves possess this property. *For all types of vector waves polarization refers to the behavior with time of one of the field vectors appropriate to that wave, observed at a fixed point in space.* [16]

Light waves are electromagnetic in nature and require four basic field vectors for their complete description: the electric field vector $\vec{E}$, the electric field displacement $\vec{D}$, the magnetic field strength $\vec{H}$ and the magnetic-flux density $\vec{B}$. Of these four vectors the *electric field strength* $\vec{E}$ is chosen to define the state of polarization of the light waves. This choice is based on the fact that when light interacts with matter, the force exerted on the electrons by the electric field of the light wave is much greater than the force exerted on these electrons by the magnetic field of the light wave. [11, 16]

2.1 Polarization of Monochromatic Waves of Arbitrary Spatial Structure

For a monochromatic wave the time variation of the electric vector $\vec{E}$ is exactly sinusoidal. At a fixed point in space the most general vibration of the electric vector $\vec{E}$ can be resolved into three independent, linear, simple-harmonic vibrations $\vec{E}_x$, $\vec{E}_y$ and $\vec{E}_z$ along three mutually orthogonal directions x, y, and z, respectively.

$$\vec{E} = \vec{E}_x\hat{x} + \vec{E}_y\hat{y} + \vec{E}_z\hat{z} \tag{2.1.1}$$

with

$$E_i = \tilde{E}_i \cos(\omega t + \delta_i) \tag{2.1.2}$$

where $\hat{x}$, $\hat{y}$ and $\hat{z}$ are unit vectors along the coordinate axes; $\tilde{E}_i$ and δ_i represent the amplitude and phase, respectively, of the linear vibration along the ith coordinate axis and ω represents the angular frequency.

It is simple to see that if a vector is drawn from a fixed observation point as an origin to represent the instantaneous electric vector $\vec{E}$, the end-point of that vector will trace an ellipse in space. Such an ellipse is periodically described at a repetition rate equal to the optical frequency $f = \frac{\omega}{2\pi}$.

2.1.1 Elliptical Polarization

A light wave whose electric vector at a fixed point in space traces the same ellipse in a regular repetitive fashion is described as elliptically polarized at that point. Elliptical (elliptic) polarization is the most general state of polarization of any optical field that is strictly monochromatic.

For complete specification of the elliptical polarization we need to know [16]

(1) The orientation in space of the plane of the ellipse of polarization;

(2) The orientation of the ellipse in its plane, its shape and sense in which it is described;

(3) The amplitude (size) of the ellipse;

(4) The absolute temporal phase.

The orientation in space of the plane of the ellipse of polarization can be specified by the unit vector $\vec{n}$, directed normal to that plane. For a monochromatic wave of arbitrary spatial structure, there are two distinct possible choices of the unit normal, either $\hat{n}$ or $-\hat{n}$. In other words, the sense of the unit normal has to be defined. Because we will be interested in travelling wave, the sense of $\hat{n}$ is uniquely and unambiguously defined parallel to the direction of propagation (direction of the average energy flow). The ellipse of polarization in its plane is determined by the following parameters.

(1) The *azimuth angle* θ is the angle between the major axis of the ellipse and the positive direction of x-axis and defined the orientation of the ellipse in its plane. All physically distinguishable azimuth can be obtained by limiting θ to the range

$$-\frac{1}{2}\pi \leq \theta \geq \frac{1}{2}\pi. \tag{2.1.3}$$

(2) The *ellipticity* e is the ratio of the length of the semi-minor axis of the ellipse b to the length of its semi-major axis a,

$$e = \frac{b}{a}. \tag{2.1.4}$$

(3) The *handedness* of the ellipse of polarization determines the sense in which the ellipse is described. It is a parameter that can assume only one of two discrete values. The polarization is right handed if the ellipse is traversed in a clockwise sense when looking against the direction of $\hat{n}$ (this means looking "into the beam" for a travelling wave). The polarization is left handed if the ellipse is traversed in a counter clockwise

sense when looking against the direction of $\hat{n}$.

Some times it is convenient to define the ellipticity in terms of handedness by allowing the ellipticity to assume positive and negative values to correspond to right handed and left handed polarization, respectively. From Eq. (1.1.4) and the use of this notation, all physically distinguishable ellipticity values can be obtained by limiting e to the range

$$-1 \leq e \leq 1. \tag{2.1.5}$$

(4) The *amplitude* (size) of an elliptical vibration can be conveniently defined in terms of the length a and b of the semi-major and semi-minor axes as

$$A = (a^2 + b^2)^{\frac{1}{2}}. \tag{2.1.6}$$

The amplitude A, defined by Eq. (2.1.6), is a measure of the strength of the elliptical vibration and its square is proportional to the energy density of the wave at the point of observation of the field.

(5) The *absolute phase* δ determines the angle between the initial position of the electric vector at $t = 0$ and the major axis of the ellipse. All possible values of the absolute phase δ will be limited to the range

$$-\pi \leq \delta \geq \pi. \tag{2.1.7}$$

2.1.2 Linear And Circular Polarizations

The circular and linear state of polarizations are special cases of the more general state of elliptical polarization and are generated when the ellipticity e assumes the special values of ± 1 and zero, respectively. The values $e = +1$ and $e = -1$ correspond to the *right-handed* and *left-handed circularly polarized state*, respectively, and when $e = 0$ the light wave is *linearly polarized.*

2.2 Jones Vector

Jones vector is a complex vector which contains complete information about the amplitude and phases of the field components, hence about the polarization of the wave. In order to understand what Jones vector means, let's take the simple case of Jones vector of a uniform TE plane wave.

2.2.1 The Jones Vector of a Uniform TE Plane Wave

For the sake of generality, we assumed in the previous sections that the time-harmonic light wave has an arbitrary spatial structure. A special case of great interest is that of a uniform TE (transverse electric) travelling plane wave. The electric field of a linearly polarized wave of this type varies with position $\vec{r}$ and time t according to

$$E(\vec{r},t) = [\tilde{E}\cos(\omega t - \vec{k}.\vec{r})]\hat{u} \tag{2.2.1}$$

$$\hat{u}.\hat{u} = 1, \hat{u}.\vec{k} = 0$$

$\hat{u}$ represents a constant unit vector in the direction of the linear polarization, transverse (orthogonal) to the direction of wave propagation given by the constant wave vector $\vec{k}$. $\tilde{E}$ is the amplitude of oscillation which is independent of $\vec{r}$ and t. The state of polarization of this can be generalized from linear to elliptic by the superposition of two linearly polarized waves of different polarizations and phases. Thus Eq. (2.2.1) can be generalized to become

$$\vec{E}(\vec{r},t) = [\tilde{E}\cos(\omega t - \vec{k}.\vec{r} + \delta)]\hat{u} + [\tilde{E}'\cos(\omega t - \vec{k}.\vec{r} + \delta')]\hat{u'} \tag{2.2.2}$$

$$\hat{u}.\hat{u} = \hat{u'}.\hat{u'} = 1, \hat{u}.\hat{u'} = \hat{u'}.\vec{k} = \hat{u}.\vec{k} = 0$$

Equation (2.2.2) describes a uniform TE elliptically polarized plane wave. $\hat{u}$ and $\hat{u'}$ represent two orthogonal unit vectors in the wave fronts along which the electric vector

is resolved into components of amplitude $\tilde{E}$ and $\tilde{E}'$ and phases δ and δ' respectively. If such a wave is assumed to propagate along the positive direction of the z axis of an xyz orthogonal, right-handed Cartesian coordinate system and if, in addition, the unit vectors $\hat{u}$ and $\hat{u'}$ are chosen parallel to the positive directions of the x and y axes, Eq. (1.4.2) becomes

$$\vec{E}(z,t) = [\tilde{E}_x \cos(\omega t - \frac{2\pi z}{\lambda} + \delta_x)]\hat{x} + [\tilde{E}_y \cos(\omega t - \frac{2\pi z}{\lambda} + \delta_y)]\hat{y}. \tag{2.2.3}$$

In Eq. (2.2.3) $\tilde{E}_x$ and $\tilde{E}_y$ represent the amplitudes of the linear, simple harmonic oscillations of the electric field components along the x and y axes, and δ_x and δ_y represent the respective phases of these oscillations. $\hat{x}$ and $\hat{y}$ are the unit vectors in the positive directions of the x and y axes. In considering the wave polarization and its modification by an optical device, we do not need the full expression of the wave given by Eq. (2.2.3). It is therefore important to seek a more concise mathematical description for the wave. [16] We achieve this result through stapes.

(1) First, once the fixed unit vectors $\hat{x}$ and $\hat{y}$ of the linearly polarized components of the wave have been chosen, there is no need to retain these unit vectors in the mathematical expression of the wave. This can be achieved by grouping the scalar (non-vector) components in the form of a 2x1 column vector matrix as follows:

$$\vec{E}(z,t) = \begin{pmatrix} \tilde{E}_x \cos(\omega t - \frac{2\pi z}{\lambda} + \delta_x) \\ \tilde{E}_y \cos(\omega t - \frac{2\pi z}{\lambda} + \delta_y) \end{pmatrix}. \tag{2.2.4}$$

The reverse step from Eq. (2.2.4) to the full expression of Eq. (2.2.3) is to multiply the element in the 1, 1 matrix position of Eq. (2.2.4) by $\hat{x}$, the element in the 2, 1 matrix position by $\hat{y}$ and to add the results.

(2) Because the field components at all points in space for a monochromatic field are known to oscillate sinusoidally with time at the same frequency, such temporal information can also be suppressed. Using the phasor notation, Eq. (2.2.3) can be

replaced by

$$\vec{E}(z) = e^{\frac{-i2\pi z}{\lambda}} \begin{pmatrix} \tilde{E}_x e^{i\delta_x} \\ \tilde{E}_y e^{i\delta_y} \end{pmatrix}. \tag{2.2.5}$$

The reverse step from Eq. (2.2.5) to Eq. (2.2.3) is to multiply the former by $e^{i\omega t}$ and take the real part of the product

$$\vec{E}(z,t) = Re[\vec{E}(z)e^{i\omega t}]. \tag{2.2.6}$$

The final step towards the desired mathematical description of a uniform TE plane wave is to drop the *spatial* information about the wave by considering the field over one fixed transverse plane for example $z = 0$ of the xyz coordinate system. If $z = 0$ is substituted in Eq. (2.2.5), we obtain

$$\vec{E}(0) = \begin{pmatrix} \tilde{E}_x e^{i\delta_x} \\ \tilde{E}_y e^{i\delta_y} \end{pmatrix}. \tag{2.2.7}$$

The reverse step from Eq. (2.2.7) to Eq. (2.2.5) (that restores the space dependence) is to multiply the former by $e^{\frac{-i2\pi z}{\lambda}}$

$$\vec{E}(z) = e^{\frac{-i2\pi z}{\lambda}} \vec{E}(0). \tag{2.2.8}$$

The vector $\vec{E}(0)$ of Eq. (2.2.7) is the desired concise representation of a single plane wave *which is known to be monochromatic, uniform and transverse-electric.* This vector is called the *Jones vector* of the wave. [16] From the Jones vector $\vec{E}(0)$ we can reconstruct the time and space dependence of the entire wave by combining Eqs. (2.2.6) and (2.2.8)

$$\vec{E}(z,t) = Re[\vec{E}(0)e^{i(\omega t - \frac{2\pi z}{\lambda})}]. \tag{2.2.9}$$

The full expression of the wave Eq. (2.2.3) can be retained by reintroducing the unit vectors $\hat{x}$ and $\hat{y}$ as explained in step 1 above.

Note that The Jones vector is not a vector in the real physical space, rather it is a vector in an abstract mathematical space formed by all the vectors that are obtained by considering all possible pairs of complex numbers for E_x and E_y.

2.2.2 Jones Vector of Some State of Polarization

For arbitrary wave let us allow the phasor components E_x and E_y of the Jones vector to assume all possible values as two independent complex numbers so that all possible state of polarization of all possible values of amplitude and phase are generated. The simplified notation of the Jones vector of this wave is

$$\vec{E} = \begin{pmatrix} E_x \\ E_y \end{pmatrix} \tag{2.2.10}$$

where

$$E_x = |E_x|e^{i\delta_x}, E_y = |E_y|e^{i\delta_y}, \tag{2.2.11}$$

and the dependence on z will be indicated when the need arises.

(1) The Jones vector of a linearly polarized wave whose electric vector executes a simple-harmonic oscillation along the x axis with unit amplitude ($A = 1$) and zero phase ($\delta = 0$) is given by

$$E_x = \begin{pmatrix} 1 \\ 0 \end{pmatrix}. \tag{2.2.12}$$

Similarly the Jones vector

$$E_y = \begin{pmatrix} 0 \\ 1 \end{pmatrix} \tag{2.2.13}$$

represents a linearly polarized wave whose electric vector executes a simple-harmonic oscillation along the y axis with unit amplitude and zero phase.

(2) For an arbitrary linearly polarized light wave, the electric vector oscillates along a general direction x' in the wave front, inclined to the fixed direction of the x axis by an azimuth angle α. For such a wave, the Jones vector is given by

$$E_{x'} = \begin{pmatrix} \cos\alpha \\ \sin\alpha \end{pmatrix} \tag{2.2.14}$$

where the linear oscillation is again of unit amplitude and zero phase. The state of linear polarization that is orthogonal to the state represented by Eq. (2.2.14) can be

obtained by the substitution $\alpha \rightarrow \alpha - \frac{1}{2}\pi$

$$E_{y'} = \begin{pmatrix} \sin\alpha \\ -\cos\alpha \end{pmatrix}. \tag{2.2.15}$$

Note that the orthogonal pair E_x and E_y of Eqs. (2.2.12) and (2.2.13) is a special case of the orthogonal pair $E_{x'}$ and $E_{y'}$ of Eqs. (2.2.14) and (1.4.15) by setting $\alpha = 0$. (3) for a pair of orthogonal waves of the left-and right-circularly polarized waves their respective Jones vectors are given by

$$E_\ell = \frac{1}{\sqrt{2}} \begin{pmatrix} 1 \\ -i \end{pmatrix}, \tag{2.2.16}$$

and

$$E_r = \frac{1}{\sqrt{2}} \begin{pmatrix} 1 \\ i \end{pmatrix}. \tag{2.2.17}$$

The linear oscillation along the x and y coordinate axes from which E_ℓ and E_r are constructed arc of equal amplitude $(\frac{1}{\sqrt{2}})$ and are in time-quadrature with one another. In the case of the left-circular state the y component *lags* the x component by a phase of $\frac{1}{2}\pi$, where as for the right-circular state the y component *leads* the x component by $\frac{1}{2}\pi$. Generally, the circular polarization is the sum of the right and left circularly polarized light waves, which is the sum of Eqs. (2.2.16) and (2.2.17) so that the Jones matrix of circularly polarized wave is

$$E_{cir} = \frac{1}{\sqrt{2}} \begin{pmatrix} 2 \\ 0 \end{pmatrix}. \tag{2.2.18}$$

2.3 Jones Matrix

Consider a uniform monochromatic TE plane wave incident on a nondepolarizing optical system that consists of either a single optical device or successive series of devices. As a result of interaction between the incident wave and the optical system one

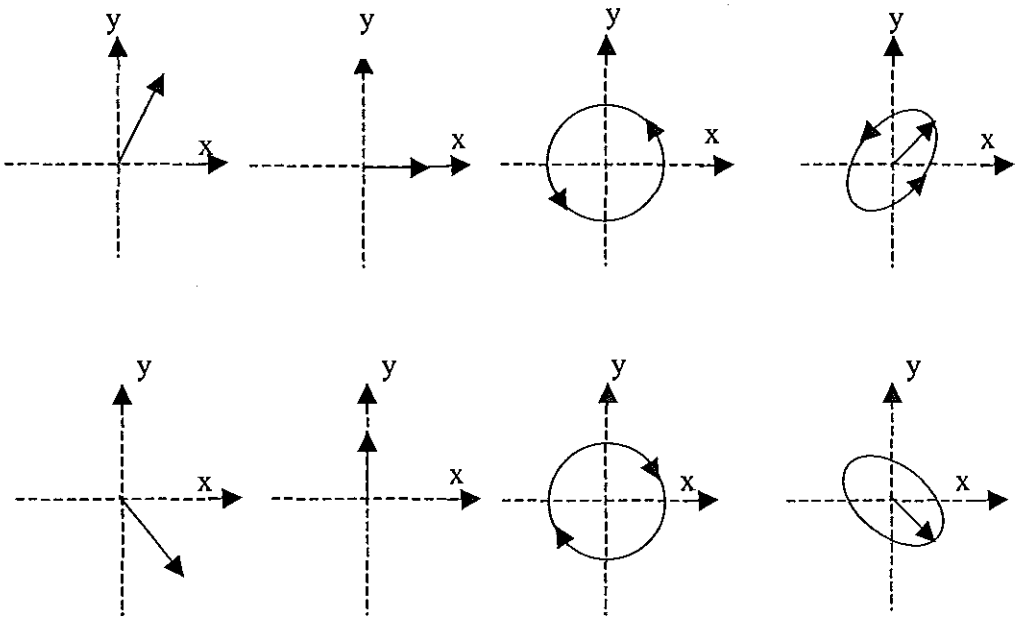

Figure 2.1: *The Jones vector of some state of polarization*

or more modified plane waves emerge from the system. Figure 2.2 shows a systematic diagram of the optical system, the incident wave and the outgoing (emergent) modified plane waves. Two space-fixed right handed Cartesian coordinate systems (x, y, z) and (x', y', z') are associated with the incident and the outgoing plane waves, with the direction z and z' taken parallel to their wave-vectors $\vec{k}$ and $\vec{k}'$, respectively. ($\vec{k}$ and $\vec{k}'$ need not be parallel.) The transverse (x, y) and (x', y')coordinate axes at the input and output of the optical system may have any suitable azimuthal orientation around the incident and the outgoing wave-vectors $\vec{k}$ and $\vec{k}'$, respectively. Let the incident and the outgoing plane waves be described by their appropriate Jones vectors E_i and E_o, referenced to the input and the output coordinate systems, respectively. As explained in §2.2, the input Jones vector E_i is a complex 2×1 column vector whose elements (phase components) E_{ix} and E_{iy} represent the sinusoidal oscillations

of the Cartesian projections of the electric vector of the incident light wave along the transverse x and y coordinate axes, respectively. Similarly the elements $E_{ox'}$ and $E_{oy'}$ of the output Jones vector E_o represent the sinusoidal oscillations of the Cartesian projections of the electric vector of the outgoing light wave along the transverse x' aud y' coordinate axes, respectively. The pair of oscillations $E_{ox'}$ and $E_{oy'}$ at the

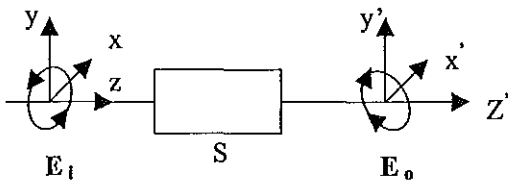

Figure 2.2: *$\vec{E}_i$ and $\vec{E}_o$ are the respective Jones vectors of plane waves incident on and emergent from the optical system S.*

output of the optical system are related to the pair of oscillations E_{ix} and E_{iy} at the input of the optical system by the following linear relations

$$E_{ox'} = T_{11}E_{ix} + T_{12}E_{iy} \tag{2.3.1}$$

$$E_{oy'} = T_{21}E_{ix} + T_{22}E_{iy}. \tag{2.3.2}$$

Eqs. (2.3.1) and (2.3.2) can be combined in the matrix form as

$$\begin{pmatrix} E_{ox'} \\ E_{oy'} \end{pmatrix} = \begin{pmatrix} T_{11} & T_{12} \\ T_{21} & T_{22} \end{pmatrix} \begin{pmatrix} E_{ix} \\ E_{iy} \end{pmatrix}, \tag{2.3.3}$$

or, more concisely,

$$\vec{E}_o = T\vec{E}_i \tag{2.3.4}$$

where

$$T = \begin{pmatrix} T_{11} & T_{12} \\ T_{21} & T_{22} \end{pmatrix}. \tag{2.3.5}$$

Eq. (2.3.4) express the law of interaction between the incident wave and the optical system as a simple linear matrix transformation of the Jones-vector representation of the wave vector. *This is the fundamental step upon which the entire Jones-matrix formulation is based.* The 2×2 transformation matrix T is called the *Jones matrix* of the optical system (or the optical device) [18] and its elements T_{ij} are, in general, complex.

2.3.1 The significance of the elements T_{ij} of the Jones matrix

The Jones matrix T describes the overall effect of the optical system on the incident wave. It is interesting to examine the meaning of each individual element T_{ij} of this Jones matrix. According to Eqs. (2.3.1) and (2.3.2), if the incident plane wave is linearly polarized with its electric vector vibrating along the x axis ($i.e. E_{iy} = 0$), the elements T_{11} and T_{21} are given by

$$T_{11} = [\frac{E_{ox'}}{E_{ix}}]_{E_{iy}=0} \tag{2.3.6}$$

$$T_{21} = [\frac{E_{oy'}}{E_{ix}}]_{E_{iy}=0} \tag{2.3.7}$$

The linear oscillation E_{ix} of the incidence electric vector along the x coordinate axis at the input of the system has produced two orthogonal linear oscillations $E_{ox'}$ and $E_{oy'}$ along the x' and y' coordinate axes at the output of the system, respectively. If, instead of being linearly polarized along the x, the incident wave is linearly polarized along the y axis, the element T_{12} and T_{22} are determined from Eqs. (2.3.1) and (2.3.2) by

$$T_{12} = [\frac{E_{ox'}}{E_{iy}}]_{E_{ix}=0} \tag{2.3.8}$$

$$T_{22} = [\frac{E_{oy'}}{E_{iy}}]_{E_{ix}=0}. \tag{2.3.9}$$

In this case the linear vibration E_{iy} has generated two orthogonal linear vibrations $E_{ox'}$ and $E_{oy'}$ at the output of the system. Generally, we can see from Eq. (2.3.6) to

Eq. (2.3.9) the diagonal elements T_{11} and T_{22} of the Jones matrix of the optical system are determined by the $x \rightarrow x'$ and $y \rightarrow y'$ input-to-output mappings of "similar" linear polarizations, whereas the off-diagonal elements T_{21} and T_{12} are determined by the $x \rightarrow y'$ and $y \rightarrow x'$ input-to-output mappings of "crossed" linear polarizations, respectively.

2.3.2 Jones matrices of reflection-type devices

When a light wave interacts with a material medium it gets modified by transmission and reflection from the surface of medium (isotropic or anisotropic). Here we are interested on the modification due to reflection. The simplest reflection-type device is one in which the wave bounces from the a single interface between two dissimilar media. If the incident plane wave has an electric vibration parallel p to the plane of incidence, the reflected wave will also have an electric vibration parallel to the plane of incidence. [18] Likewise, an an electric vibration perpendicular s to the plane of incidence is reflected into a similar vibration perpendicular to the plane of incidence. By resolving the incident E_i and reflected E_r electric vectors along the p and s directions, the effect of reflection can be expressed as

$$E_r = RE_i, \tag{2.3.10}$$

where the reflection Jones matrix is given by

$$R = \begin{pmatrix} R_{pp} & 0 \\ 0 & R_{ss} \end{pmatrix} \tag{2.3.11}$$

The $p \rightarrow p$ and $s \rightarrow s$ diagonal reflection coefficients R_{pp} and R_{ss} are given by Fresnel formulae and both are, in general complex. For the two eigenpolarizations of linear vibrations parallel (p) and perpendicular (s) to the plane of incidence, the associated eigenvalues, let V_{ex} and V_{ey}, become the complex-amplitude reflection coefficients R_{pp}

and R_{ss}, respectively

$$\begin{aligned} V_{ex} &= R_{pp} \\ V_{ey} &= R_{ss} \end{aligned}, \tag{2.3.12}$$

Then its Jones matrix become

$$R = |V_{ey}| \begin{pmatrix} \rho & 0 \\ 0 & 1 \end{pmatrix}, \tag{2.3.13}$$

where

$$\rho = \frac{V_{ex}}{V_{ey}} = \frac{R_{pp}}{R_{ss}}$$

is the ratio of the eigenvalues of the p and s components of the field. The matrix given by Eq. (2.3.13) is the reflection Jones matrix of the optical system. Following the same procedure, the Jones matrices of an ideal linear polarizer and analyzer (ideal polarizer is one which does not absorb), can be written as

$$T_P = \begin{pmatrix} 1 & 0 \\ 0 & 0 \end{pmatrix} \tag{2.3.14}$$

and

$$T_A = \begin{pmatrix} 1 & 0 \\ 0 & 0 \end{pmatrix}, \tag{2.3.15}$$

because only component of light parallel to the transmission axis is allowed to pass through.

Chapter 3

THEORY AND ANALYSIS OF MEASUREMENTS IN ELLIPSOMETRY SYSTEMS

3.1 Introduction

This chapter describes the use of ellipsometry for measurement of the change of the state of polarization of a polarized light wave. It is a non-invasive and non-destructive technique which requires low-power light source and does not affect most of the measurement processes there by it renders ellipsometry as a convenient tool for measurement of *in situ* studies. [10] Generally, Ellipsometry is conducted in order to obtain "information" about an "optical system" which modifies the state of polarization such as the R.I, the thickness, etc. of semi-transparent thin films and dielectric crystals. The materials may be in the liquid or solid phase, may be optically isotropic or anisotropic, and can be either in bulk or thin film form. The instrument relies on the fact that the reflection at the dielectric interface depends on the polarization of the light while the transmission of light through a transparent layer changes the phase of the incoming wave depending on the R.I of the material. Depending upon the prevalent mode of interaction, this method can be divided in three parts: (i)

Reflection Ellipsometry (ii) Transmission Ellipsometry (iii) Scattering Ellipsometry. We have used reflection ellipsometry in our measurement which is discussed in the following section.

3.2 Reflection Ellipsometry

Reflection ellipsometry is a technique based on measurements of the state of polarization of the incident and reflected waves, leading to the determination of the ratio ρ of the complex Fresnel reflection coefficients for the p and s polarization [1, 8]

$$\rho = \frac{r_p}{r_s}.$$

When a light wave is reflected or refracted at the interface between two optically dissimilar media, the state of polarization is changed abruptly. [19] Such a change is caused by the difference in the Fresnel reflection and transmission coefficients for the two linear polarizations p and s. The reflection ellipsometry can be performed either by rotating the analyzer or static photometric means. We have used Rotating Analyzer Ellipsometry (RAE) technique in our studies where the polarizer angle P is kept fixed and the intensity I of the light wave reflected from the sample is measured as a function of analyzer angle A. The azimuth angle of the analyzer is rotated from 0^0 to 360^0. The values of Ψ and Δ are obtained from the intensity verses analyzer angle graph. The ratio ρ of complex Fresnel reflection coefficients for the p and s polarization as mentioned in Eq. (2.2.48), is used to get an expression for the R.I of a material.

$$\rho = \frac{r_p}{r_s} = \tan\Psi e^{i\Delta}.$$

If we substitute the respective magnitude values of $\hat{r}_p$ and $\hat{r}_s$ in Eq. (2.2.48) from Eqs. (2.2.22) and (2.2.28), we get

$$|\hat{\rho}| = \frac{|\hat{r}_p|}{|\hat{r}_s|} = \frac{n_1\cos\theta_o - n_o\cos\theta_1}{n_1\cos\theta_o + n_o\cos\theta_1} \times \frac{n_o\cos\theta_o - n_1\cos\theta_1}{n_o\cos\theta_o + n_1\cos\theta_1}. \tag{3.2.1}$$

Let $\frac{n_1}{n_o} = n$. Then after a few steps Eq. (3.2.1) becomes

$$(n^2 - 1)(1 + \rho)\cos\theta_o \cos\theta_1 + n(1 - \rho)(\cos^2\theta_o - \cos^2\theta_1) = 0. \tag{3.2.2}$$

Making use of Snell's law one can write

$$\cos\theta_1 = [1 - \frac{\sin^2\theta_o}{n^2}]^{1/2} \tag{3.2.3}$$

and using Eq. (3.2.3) into Eq. (3.2.2) for $\cos\theta_1$, Eq. (3.2.2) will take the form

$$n = \sin\theta_o[1 + (\frac{1-\rho}{1+\rho})^2 \tan^2\theta_o]^{1/2}$$

or

$$n_1 = n_o \sin\theta_o[1 + (\frac{1-\rho}{1+\rho})^2 \tan^2\theta_o]^{1/2}. \tag{3.2.4}$$

Hence the measurement of the ratio ρ and the incident angle θ_o from the reflection ellipsometer technique enables us to calculate the R.I of the material under investigation. Please remember from §2.1 that the general expression for the refractive index of any material medium has two parts

$$n = n_o + i\kappa$$

where n_o and κ are the real and imaginary parts of the refractive index, respectively, and κ is to be determined from the material absorption coefficient.

3.3 Derivation of Ellipsometer Equations

A well-collimated beam of monochromatic linearly polarized light from a suitable source is passed through the polarizing section of the instrument. The polarizer is set at azimuth angle P from the x-axis of the Cartesian coordinate system. That means the transmission axis of the polarizer makes an angle P from the x-axis of the Cartesian coordinate of the light. Here in after-wards the following notation will

be used. Letter superscripts denote the coordinate system with respect to which a Jones vector or matrix is referenced. The first letter of a subscript identifies an optical component, the second either its *input* or *output*. For example, E^{te}_{Po} is the Jones vector (electric field) of the light beam at the output of the polarizer in its transmission-extinction frame of reference. Then the light incident on the polarizer in the Cartesian coordinate frame is given by:

$$E^{xy}_{Pi} = \begin{pmatrix} \cos P & \sin P \\ -\sin P & \cos P \end{pmatrix} \begin{pmatrix} E_x \\ E_y \end{pmatrix}. \tag{3.3.1}$$

Or

$$E^{xy}_{Pi} = \begin{pmatrix} E_x \cos P + E_y \sin P \\ -E_x \sin P + E_y \cos P \end{pmatrix}. \tag{3.3.2}$$

After the light passes through the polarizer, only component of light parallel to the transmission axis of the polarizer will come out. Component of the light parallel to the extinction axis will be blocked. In the transmission-extinction axis, the electric field which comes out from the polarizer is

$$E^{te}_{Po} = \begin{pmatrix} E^{t}_{po} \\ E^{e}_{po} \end{pmatrix}. \tag{3.3.3}$$

In terms of the Jones matrix of the polarizer and the incident wave (Eq. (3.3.2)) Eq. (3.3.3) can be written as

$$E^{te}_{Po} = T^{te}_{P} E^{xy}_{Pi}. \tag{3.3.4}$$

Using Eq. (3.3.2), Eq. (3.3.4) becomes

$$E^{te}_{Pi} = \begin{pmatrix} 1 & 0 \\ 0 & 0 \end{pmatrix} \begin{pmatrix} E_x \cos P + E_y \sin P \\ -E_x \sin P + E_y \cos P \end{pmatrix}. \tag{3.3.5}$$

Or

$$E^{te}_{Po} = \begin{pmatrix} E_x \cos P + E_y \sin P \\ 0 \end{pmatrix} = A_P \begin{pmatrix} 1 \\ 0 \end{pmatrix}. \tag{3.3.6}$$

Where

$$T_p^{te} = \begin{pmatrix} 1 & 0 \\ 0 & 0 \end{pmatrix}$$

is the Jones matrix of the polarizer, Eq. (2.3.14), and

$$A_P = E_x \cos P + E_y \sin P \tag{3.3.7}$$

is the amplitude of the transmitted light wave. This light wave transmitted from the polarizer will incident on the optical system (sample) and can be written in Cartesian coordinate frame. This is done by counter-rotation of the light wave given by Eq. (3.3.6) for angle P. then

$$E_{Si}^{xy} = R(-P)E_{Po}^{te}. \tag{3.3.8}$$

$$E_{Si}^{xy} = A_P \begin{pmatrix} \cos P & -\sin P \\ \sin P & \cos P \end{pmatrix} \begin{pmatrix} 1 \\ 0 \end{pmatrix}. \tag{3.3.9}$$

Or

$$E_{Si}^{xy} = A_P \begin{pmatrix} \cos P \\ \sin P \end{pmatrix}. \tag{3.3.10}$$

Where

$$R(-P) = \begin{pmatrix} \cos P & -\sin P \\ \sin P & \cos P \end{pmatrix} \tag{3.3.11}$$

is the counter-rotation matrix. This light, Eq. (3.3.11), will be reflected from the sample aud the Jones vector of this reflected light wave is related to that at its input by

$$E_{So}^{xy} = R_S^{xy} E_{Si}^{xy}. \tag{3.3.12}$$

The optical system under investigation has orthogonal linear eigenpolarizations (V_{ex} and V_{ey})along orthogonal coordinate axes x and y so that the Jones matrix R_S^{xy} is diagonal and given by Eq. (2.3.13)

$$R_S^{xy} = \begin{pmatrix} V_{ex} & 0 \\ 0 & V_{ey} \end{pmatrix} = |V_{ey}| \begin{pmatrix} \rho & 0 \\ 0 & 1 \end{pmatrix}$$

where

$$\rho = \frac{V_{ex}}{V_{ey}} = \tan\Psi e^{i\Delta} \tag{3.3.13}$$

is the complex polarization variable, which is the ratio of the eigenvalues of the reflected light wave along the x direction to the y direction. Using Eq. (2.3.13) into Eq. (3.3.12)

$$E_{So}^{xy} = A_P|V_{ey}| \begin{pmatrix} \rho & 0 \\ 0 & 1 \end{pmatrix} \begin{pmatrix} \cos P \\ \sin P \end{pmatrix} \tag{3.3.14}$$

$$E_{So}^{xy} = \begin{pmatrix} E_{So}^{x} \\ E_{So}^{y} \end{pmatrix} = A_P|V_{ey}| \begin{pmatrix} \rho\cos P \\ \sin P \end{pmatrix}. \tag{3.3.15}$$

The light wave reflected from the sample, Eq. (3.3.15) will then be analyzed by the analyzer whose azimuth angle is A from the x axis. Then the light wave incident on the analyzer in its transmission-extinction (te) axes is

$$E_{Ai}^{te} = R(A)E_{Ai}^{xy}, \tag{3.3.16}$$

but $E_{Ai}^{xy} = E_{So}^{xy}$. Then

$$E_{Ai}^{te} = A_P|V_{ey}| \begin{pmatrix} \cos A & \sin A \\ -\sin A & \cos A \end{pmatrix} \begin{pmatrix} \rho\cos P \\ \sin P \end{pmatrix}. \tag{3.3.17}$$

Or

$$E_{Ai}^{te} = A_P|V_{ey}| \begin{pmatrix} \rho\cos P\cos A + \sin P\sin A \\ -\rho\cos P\sin A + \sin P\cos A \end{pmatrix} \tag{3.3.18}$$

where

$$R(A) = \begin{pmatrix} \cos A & \sin A \\ -\sin A & \cos P \end{pmatrix} \tag{3.3.19}$$

is the rotation matrix of the analyzer. The light wave emergent from the analyzer is related to that at its input by

$$E_{Ao}^{te} = T_A^{te} E_{Ai}^{te} \tag{3.3.20}$$

where T_A^{te} is the Jones matrix of the analyzer, like Eq. (2.3.14) is for the polarizer, and given by Eq. (2.3.15)

$$T_A^{te} = \begin{pmatrix} 1 & 0 \\ 0 & 0 \end{pmatrix}$$

Since only the component of the light wave parallel to the transmission axis of the analyzer passes through, Eq. (3.3.20) will take the form

$$E_{Ao}^{te} = \begin{pmatrix} E_{Ao}^t \\ E_{Ao}^e \end{pmatrix} = A_P|V_{ey}| \begin{pmatrix} \rho \cos P \cos A + \sin P \sin A \\ 0 \end{pmatrix}. \tag{3.3.21}$$

This light wave, Eq. (3.3.21), emergent from the analyzer will be incident on the detector (which means the light wave at the detector is also given by Eq. (3.4.21)). The detector detects (and then amplified by the lock-In amplifier) the intensity I_D of this light wave. It is known that the intensity I_D of the detected wave is proportional to the square of the amplitude of the light wave at the detector; i.e.,

$$I_D \propto (E_D^t)^\dagger E_D^t$$

or

$$I_D = K_D|E_D^t|^2 \tag{3.3.22}$$

$$I_D = K_D|A_P|^2|V_{ey}|^2|\rho \cos P \cos A + \sin P \sin A|^2. \tag{3.3.23}$$

But ρ is a complex polarization variable given by Eq. (3.3.13) so that Eq. (3.3.23) becomes

$$I_D = G|\tan \Psi e^{i\Delta} \cos P \cos A + \sin P \sin A|^2 \tag{3.3.24}$$

where

$$G = |A_P|^2 K_D |V_{ey}|^2.$$

Equation (3.3.24) can be written as

$$I_D = G(\sin^2 P \sin^2 A + \cos^2 P \cos^2 A \tan^2 \Psi + 2 \cos P \cos A \sin P \sin A \tan \Psi \cos \Delta). \tag{3.3.25}$$

Substituting

$$\sin^2 A = \frac{1-\cos 2A}{2}, \cos^2 A = \frac{1+\cos 2A}{2}$$

$$2\sin A \cos A = \sin 2A,$$

into Eq. (3.3.25) becomes

$$I_D = G[(\frac{\sin^{2P}}{2} + \frac{\cos^2 P}{2}\tan^2) + (\frac{\cos^2 P}{2}\tan^2\Psi - \frac{\sin^2 P}{2})\cos 2A + \cos P \sin P \tan\Psi \cos\Delta \sin 2A] \tag{3.3.26}$$

or

$$I_D = G[C + \alpha^{'}\cos 2A + \beta^{'}\sin 2A]. \tag{3.3.27}$$

If I_o denotes the intensity of the light beam at the output of the optical system S, the proportion I_D of I_o passed by the analyzer A and detected by the photodetector D is

$$I_D = \bar{I}_o[1 + \alpha\cos 2A + \beta\sin 2A]. \tag{3.3.28}$$

Where $\bar{I}_o$ represents the average detected signal over one full (half) rotation of the analyzer and α and β represent the normalized cosine and sine Fourier coefficients of the signal $I_D(A)$. From Eqs. (3.3.27) and (3.3.28) the values of C, α and β are obtained from Eq. (3.3.26), and are given by

$$C = \frac{\sin^2 P}{2} + \frac{\cos^2 P}{2}\tan^2\Psi \tag{3.3.29}$$

$$\alpha = \frac{\frac{\cos^2 P}{2}\tan^2\Psi - \frac{\sin^2 P}{2}}{C}$$

$$\beta = \frac{\cos P \sin P \tan\Psi \cos\Delta}{C}.$$

The relationships between α and β with the ellipsometer parameters Ψ and Δ are given bellow. α and β, from Eq. (3.3.28), are constants to be determined by curve fitting method from the graph of intensity verses analyzer angle for Eq. (3.3.28).

$$\cos^2 P\tan^2\Psi - \sin^2 P = 2C\alpha \tag{3.3.30}$$

$$\sin P \cos P \tan \Psi \cos \Delta = C\beta. \tag{3.3.31}$$

Using the value of C from Eq. (3.3.29) into Eqs. (3.3.30) and (3.3.31) we get

$$\cos^2 P \tan^2 \Psi - \sin^2 P = (\sin^2 P + \cos^2 P \tan^2 \Psi)\alpha \tag{3.3.32}$$

and

$$2 \sin P \cos P \tan \Psi \cos \Delta = (\sin^2 P + \cos^2 P \tan^2 \Psi)\beta. \tag{3.3.33}$$

From Eq. (3.3.32)

$$\cos^2 P \tan^2 \Psi(1 - \alpha) = (1 + \alpha) \sin^2 P$$

$$\tan \Psi = \sqrt{\frac{1+\alpha}{1-\alpha}} \tan P. \tag{3.3.34}$$

Using Eq. (3.3.34) into Eq. (3.3.33) we get

$$\cos \Delta = \frac{\beta}{\sqrt{1-\alpha^2}}. \tag{3.3.35}$$

Eqs. (3.3.34) and (3.3.35) are the desired relationships between the ellipsometer parameters Ψ and Δ with the constants α and β for a given azimuth angle P of the polarizer. Thus α and β, determined by the curve fitting of Eq. (3.4.28), are used into Eqs. (3.3.34) and (3.3.35), which in turn used to determined ρ, the ratio of the complex Fresnel coefficients from Eq. (3.3.13). Once the value of ρ is determined, we can calculate the R.I of the sample using Eq. (3.2.4).

3.4 The Principle of Operation (Methodology)

In the general scheme of ellipsometry to be conducted here, a polarized light wave probe is allowed to interact with an optical system under investigation. An operational diagram of a general Ellipsometry arrangement is shown in figure 3.1. A well-collimated beam of monochromatic linearly polarized light from a suitable light source (L) is passed through a polarizing section of the instrument that consists of

a linear polarizer (P) to produce light of known controlled polarization. The light emergent from the polarizer and incident on the optical system (S) is totally polarized light whose state of polarization is controlled by the rotational azimuth angle of the polarizer. This emergent light from the polarizer interacts with the optical system under study and its polarization is modified. The modified state of polarization of the light beam outgoing from the optical system is analyzed by the analyzing section of the instrument that consists of a linear analyzer (A) followed by a photodetector (D). The photodetector D detects the light flux after the light has travelled through the Polarizer-System-Analyzer (PSA)sequences of elements. The operator changes the azimuth angles of the polarizer P and analyzer A , and measures the light intensity at different azimuths of P and A. For the polarizer and analyzer, the azimuth P and A define the orientation of their transmission axes (i,e., the direction of the transmitted linear eigenpolarizations). Here, in this study, we used two laser sources: (1) He-Ne laser source, PHYWE,Germany made of model $1125P$, Nr.:CS2236 for the production a laser light of intensity $50mW$ at wavelength $632.8nm$, and (2) A temperature tnnable Semiconductor-Diode laser source manufactured by MEOS, model LDC01 for the generations of laser lights of wavelengths $804.4nm$ at temperature 16.24^0c and $808.4nm$ at temperature 27.9^0c, respectively. The light received by the PIN photodetector is amplified for measurement by a Lock-In amplifier made by Stanford Research Systems, model SR830 DSP.

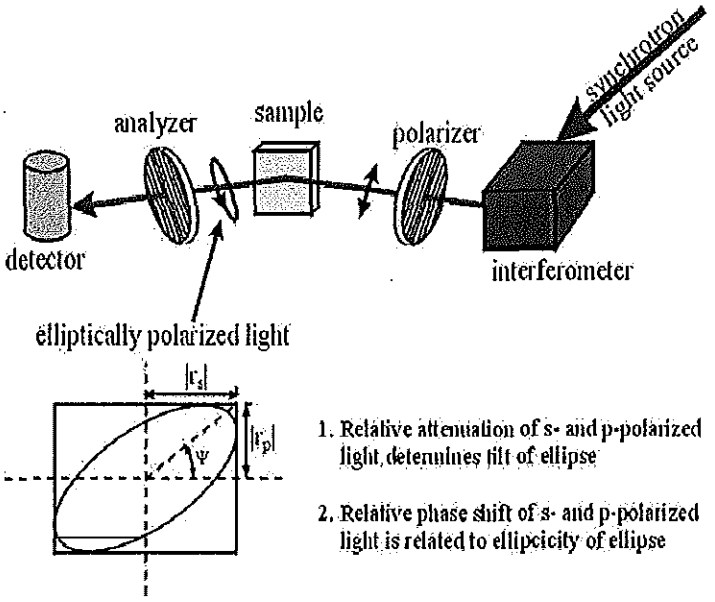

Figure 3.1: *An optical diagram of a general ellipsometry arrangement for PSA.*

Chapter 4

DATA, DATA ANALYSIS AND INTERPRETATION

4.1 Data Analysis and Interpretation

In this chapter the indices of refraction of KTP crystal are calculated using the equations we established in the previous chapters. KTP is a biaxial crystal which has two optic axes and three refractive indices: n_x, n_y and n_z. The Sellmeier equations for the refraction indices along the x, y and z axes are given in terms of the wavelength of the light. These are [12]

$$n_x^2 = 3.0065 + 0.03901/(\lambda^2 - 0.04251) - 0.01327\lambda^2 \tag{4.1.1}$$

$$n_y^2 = 3.0333 + 0.04154/(\lambda^2 - 0.04547) - 0.01408\lambda^2 \tag{4.1.2}$$

$$n_z^2 = 3.3134 + 0.05694/(\lambda^2 - 0.05658) - 0.01682\lambda^2, \tag{4.1.3}$$

where λ is in μm. Apart from the wavelength and temperature, the R.Is of the crystal depends on the direction of the polarization and the incident angle of the light wave. In order to avoid the angle dependence of the R.Is, we set the angle of incident of the

light wave near the Brewster angles for each indices at a given wavelength of the light. The intensity waveforms obtained from the ellipsometric measurement are sinusoidal in nature and are given by Eq. (3.3.28)

$$I_D = \bar{I}_o[1 + \alpha \cos 2A + \beta \sin 2A].$$

In the previous chapter the use of Fourier analysis has been discussed to obtain α and β for RAE. To this end, a graph for intensity I verses analyzer angle A is drawn from the data obtained. A theoretical model of the graph is fitted to the experimental one so that the coefficients α and β are obtained from the best graph fit to the experimental graph. These Fourier coefficients are related to the ellipsometric parameters Ψ and Δ by Eqs. (3.3.34) and (3.3.35) respectively which provide the value of ρ to calculate the R.I of KTP using Eq. (3.2.4). From the surface morphology of KTP crystal we found that out of the three faces of the crystal one of the faces is dim to detected light signals reflected (transmitted) from the surface.

Hence we only took data of the reflected light signals from the two transparent surfaces which are parallel to the x-axis and y-axis, correspondence to n_x and n_y R.Is of the KTP crystal, respectively. These data are analyzed for each wavelength of the laser and graphs are plotted for intensity verses analyzer angle (I-A). We fit the best theoretical graph (model) to our experimental one by using Microsoft Origin 6.1 software to obtain the Fourier coefficients α and β. Dotted curves indicate the experimental results and line curves indicate the fitted (model)graphs. The transmission range of KTP is from $350nm$ to $4500nm$. Figure 4.1 shows the transmission spectrum of KTP. The figure shows that KTP is high transparent in the visible to mid infrared region so that the imaginary part of the R.I which comes out of the absorption of the crystal is insignificant to be counted. As a result of this we only calculated the real part of the R.I by taking the magnitude of the complex Fresnel reflection coefficient ρ into consideration. We analyzed the data and discussed the results for each of the

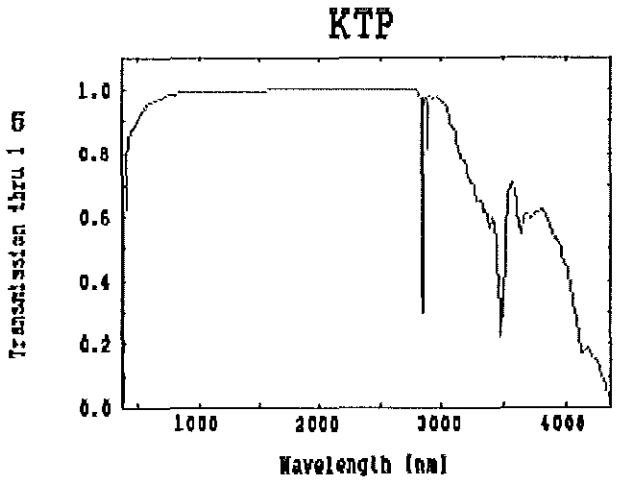

Figure 4.1: *The transmission spectrum for KTP.*

laser sources used.

He-Ne laser ($\lambda = 632.8nm$)

The I-A curves for He-Ne laser source $\lambda = 632.8nm$ are given in figures 4.2 and 4.3 and are recorded at incident angles $\theta_o = 60.4^0$, and $\theta_o = 60.6^0$, respectively. Figure 4.2 is for the n_x and figure 4.3 is for the n_y. From the figure 4.2 the calculated values of Fourier coefficients are $\alpha = 0.00159 \pm 0.00004$ and $\beta = -0.00006 \pm 0.00004$. Using these results in Eqs. (3.3.34) and (3.3.35), we get the values

$$\begin{aligned} \tan\Psi &= 1.0016 \\ \cos\Delta &= -0.00006 \end{aligned} \tag{4.1.4}$$

Using the the above results, Eq. (4.1.4), in Eq. (2.2.48) one can find

$$\rho = -6.0096 \times 10^{-5}. \tag{4.1.5}$$

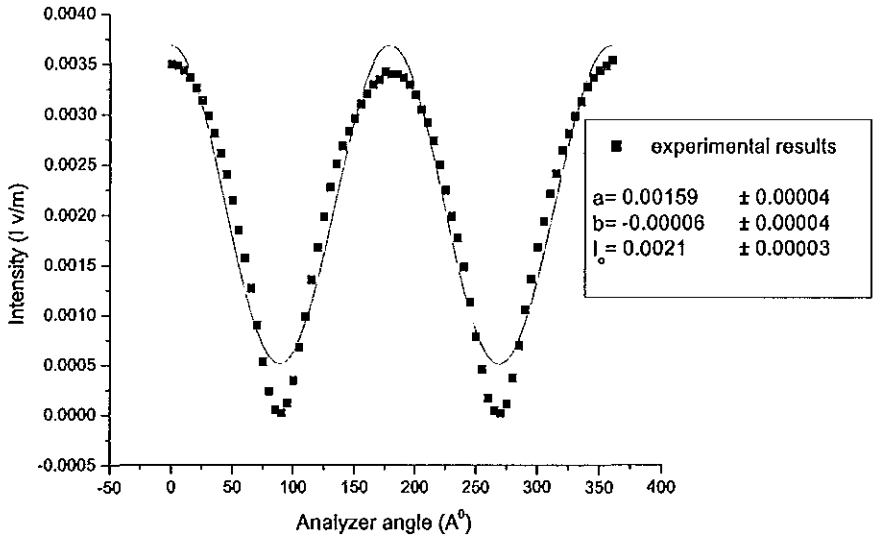

Figure 4.2: *I-A curve for n_x at wavelength $\lambda = 632.8nm$.*

This gives the R.I of of KTP crystal along the x-axis to be

$$n_x = 1.7605 \tag{4.1.6}$$

Using the Sellmeire equation, Eq. (4.1.1), the R.I n_x at $\lambda = 632.8nm$ is

$$n_x = 1.7635 \tag{4.1.7}$$

The difference Δn_x between the two results is

$$\Delta n_x = 1.7635 - 1.7605 = 0.003$$

Similarly, from figure 4.3, $\tan\Psi = 1.7333$ and $\cos\Delta = -0.00008$, which gives the R.I n_y to be

$$n_y = 1.7751 \tag{4.1.8}$$

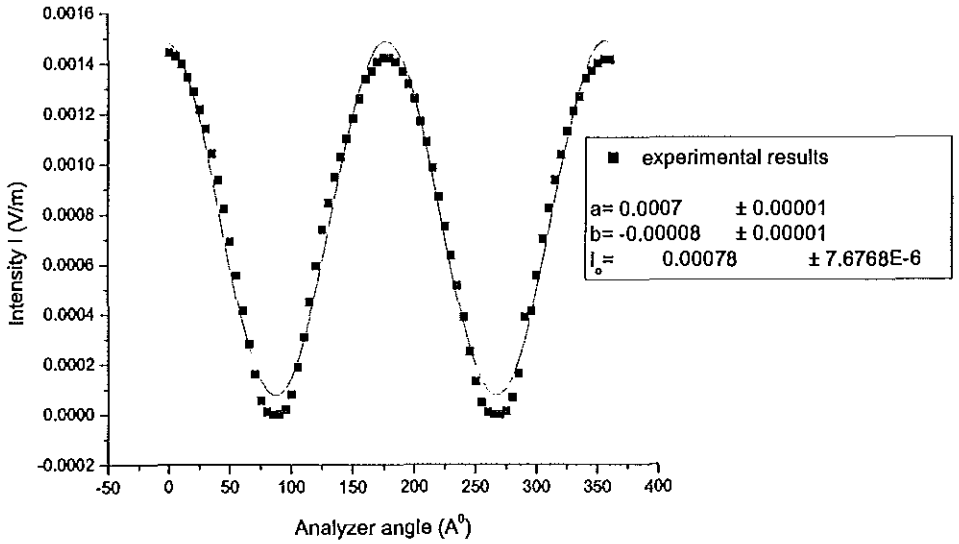

Figure 4.3: *I-A curve for n_y at wavelength $\lambda = 632.8nm$.*

Again using the Sellmeire equation, Eq. (4.1.2), the R.I n_y at $\lambda = 632.8nm$ is expected to be

$$n_y = 1.7733 \tag{4.1.9}$$

The difference between the two results is

$$\Delta n_y = 1.7751 - 1.7733 = 0.0018$$

We can see from Eqs. (4.1.6) to (4.1.9) that our results are in good agreements with the theoretical expectations.

Semiconductor: Diode laser source

a: at $\lambda = 804.4nm$

The I-A curves for Semiconductor: Diode laser source at $\lambda = 804.4nm$ are given in figures 4.4 and 4.5 at incident angle $\theta_o = 60.2^0$ and $\theta_o = 60.4^0$, respectively. The diode laser source is set at temperature 16.24^0c to produce light of wavelength $\lambda = 804.4nm$. Figure 4.4 is for the n_x and figure 4.5 is for the n_y. From figure 4.4 the values of

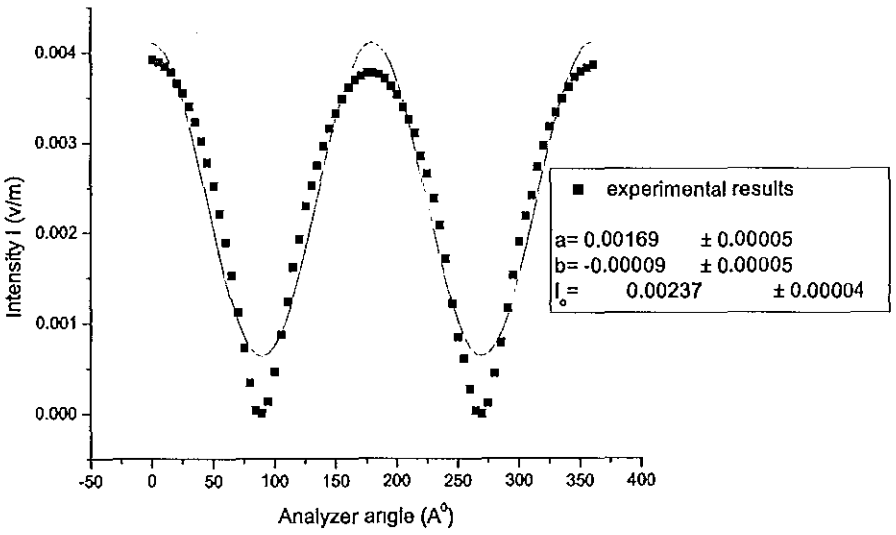

Figure 4.4: *I-A curve for n_x at wavelength $\lambda = 804.4nm$.*

Fourier coefficients are $\alpha = 0.00169 \pm 0.00005$ and $\beta = -0.00009 \pm 0.00005$ which give the value $\tan\Psi = 1.0017$, $\cos\beta = -0.00009$ and $\rho = -9.015 \times 10^{-5}$. Therefore the R.I n_x at this wavelength is

$$n_x = 1.7464 \tag{4.1.10}$$

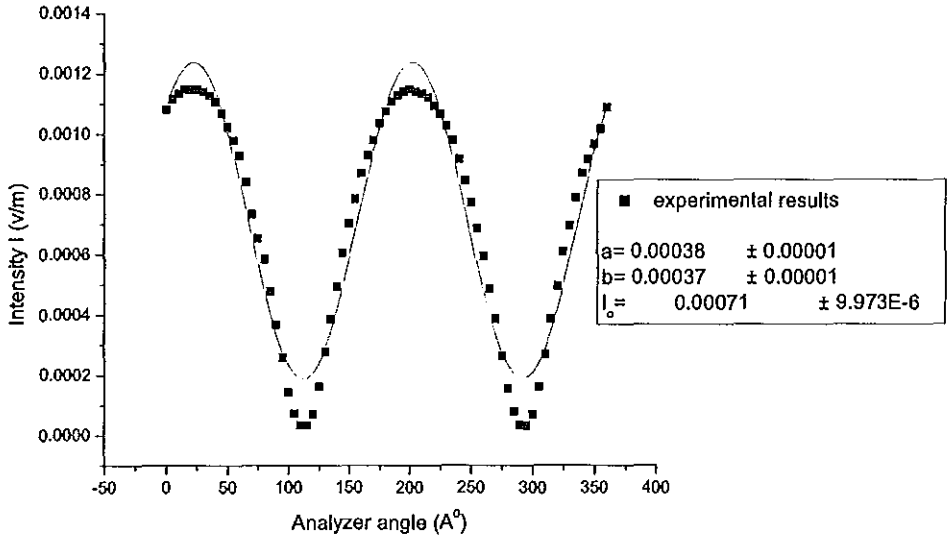

Figure 4.5: *I-A curve for n_y at wavelength $\lambda = 804.4nm$.*

Using the Sellmeire equation, Eq. (4.1.1), at wavelength $\lambda = 804.4nm$, this R.I is

$$n_x = 1.7500 \tag{4.1.11}$$

and the difference between the two results is

$$\Delta n_x = 1.75 - 1.7464 = 0.0036$$

Similarly, from figure 4.5, $\tan\Psi = 1.0004$ and $\cos\Delta = 0.00037$, which gives the R.I n_y to be

$$n_y = 1.7594 \tag{4.1.12}$$

Again using the Sellmeire equation,Eq. (4.1.2), the refractive index n_y at $\lambda = 804.4nm$ is expected to be

$$n_y = 1.7588 \tag{4.1.13}$$

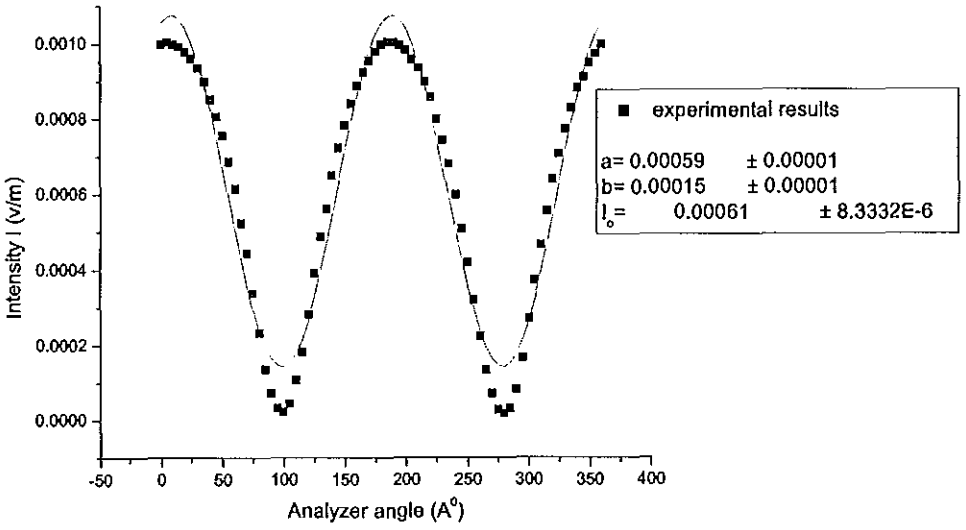

Figure 4.6: *I-A curve for n_x at wavelength $\lambda = 808.4nm$.*

which give the difference between the two to be

$$\Delta n_y = 1.7594 - 1.7588 = 0.0006$$

We can again see from Eqs. (4.1.10) to (4.1.13) that our results are in good agreements with the theoretical expectations.

b: at $\lambda = 808.4nm$

The Figures 4.6 and 4.7 show the I-A curves for the n_x and n_y, respectively, at $\lambda = 808.4nm$. The diode laser source is set at temperature 27.9^0c to produce light of the required wavelength $\lambda = 808.4nm$. From figure 4.6 the values of the Fourier coefficients are $\alpha = 0.00059 \pm 0.00001$ and $\beta = 0.00015 \pm 0.00001$ which give $\rho = -1.5009 \times 10^{-4}$ so that the R.I n_x is

$$n_x = 1.7454 \tag{4.1.14}$$

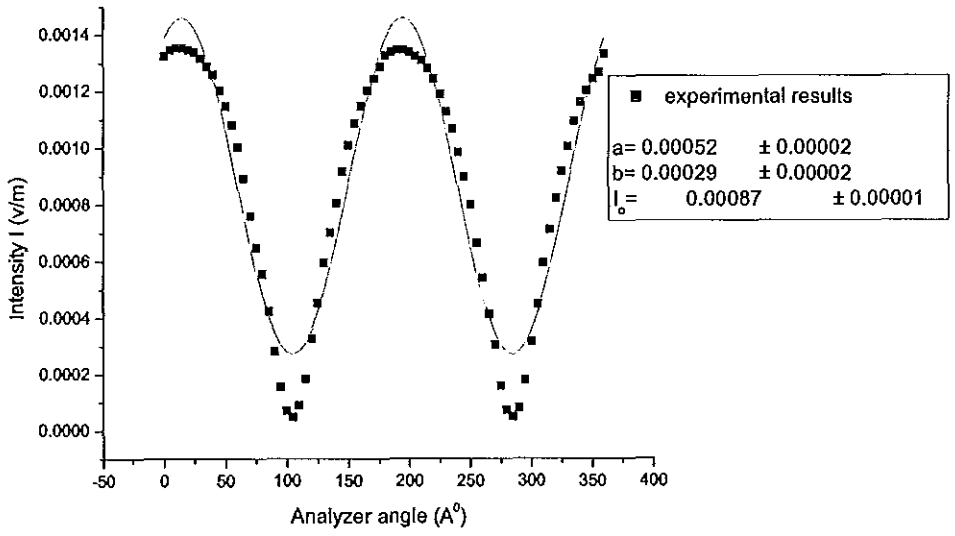

Figure 4.7: *I-A curve for n_y at wavelength $\lambda = 808.4nm$.*

and using the Sellmeire equation, Eq. (4.1.1), one can get

$$n_x = 1.7497 \tag{4.1.15}$$

and the difference between the two results is

$$\Delta n_x = 1.7497 - 1.7454 = 0.0043$$

For the n_y figure 4.7 gives $\alpha = 0.00052 \pm 0.00002$ and $\beta = 0.00029 \pm 0.00002$ which give $\rho = 2.9015 \times 10^{-4}$ so that n_y is

$$n_y = 1.7590 \tag{4.1.16}$$

and the Sellmeire equation Eq. (4.1.2), gives

$$n_y = 1.7585 \tag{4.1.17}$$

with a difference between the two results to be

$$\Delta n_y = 1.7590 - 1.7585 = 0.0005$$

All the above values reveal that our experimental results are in good agreement with the theoretical values.

4.2 Data

The data recorded from the measurement are given in tables 1 and 2 for n_x and n_y, respectively.

Table1. Data of the intensity of reflected light at each analyzer angle for n_x at incident angles $\theta_o = 60.4^0$ for wavelengths $\lambda = 632.8nm$ and $\theta_o = 60.2^0$ $\lambda = 804.4$ and $\lambda = 808.4nm$.

A^0	I at $\lambda = 632.8nm$	I at $\lambda = 804.4nm$	I at $\lambda = 808.4nm$
0	0.00349	0.00392	9.9856E-4
5	0.00348	0.00389	0.001
10	0.00343	0.00384	9.9856E-4
15	0.00336	0.00378	9.9225E-4
20	0.00326	0.00366	9.7969E-4
25	0.00314	0.00355	9.61E-4
30	0.00298	0.0034	9.3636E-4
35	0.00281	0.00323	9E-4
40	0.00261	0.00301	8.5264E-4
45	0.0024	0.00278	8.0656E-4
50	0.00214	0.00252	7.5625E-4
55	0.00185	0.00221	6.8644E-4
60	0.00157	0.00189	6.1504E-4
65	0.00127	0.00153	5.2441E-4
70	9E-4	0.00112	4.4521E-4

Continued

A^0	I at $\lambda = 632.8nm$	I at $\lambda = 804.4nm$	I at $\lambda = 808.4nm$
75	5.3361E-4	7.2361E-4	3.3856E-4
80	2.4025E-4	3.3856E-4	2.3409E-4
85	4.9E-5	3.844E-5	1.3689E-4
90	2.116E-5	4.84E-6	7.225E-5
95	1.1881E-4	1.3689E-4	3.249E-5
100	3.4596E-4	4.6225E-4	2.304E-5
105	6.76E-4	8.7025E-4	4.489E-5
110	9.8596E-4	0.00124	1.0816E-4
115	0.00135	0.00162	1.8225E-4
120	0.00167	0.00193	2.8224E-4
125	0.00198	0.00229	3.9204E-4
130	0.00228	0.00252	4.8841E-4
135	0.00251	0.00275	5.6169E-4
140	0.00268	0.00296	6.5025E-4
145	0.00283	0.00316	7.2361E-4
150	0.00296	0.00332	7.84E-4
155	0.0031	0.00348	8.41E-4
160	0.0032	0.0036	8.8804E-4
165	0.00329	0.00368	9.2416E-4
170	0.00334	0.00373	9.5481E-4
175	0.00342	0.00377	9.7969E-4
180	0.0034	0.00377	9.9856E-4
185	0.0034	0.00376	0.001
190	0.00336	0.00371	0.001
195	0.00329	0.00362	9.9856E-4
200	0.00319	0.00353	9.8596E-4
205	0.00305	0.00339	9.61E-4

Continued

A^0	I at $\lambda = 632.8nm$	I at $\lambda = 804.4nm$	I at $\lambda = 808.4nm$
210	0.00292	0.00325	9.3636E-4
215	0.00274	0.0031	9E-4
220	0.0025	0.00285	8.5849E-4
225	0.00225	0.00265	8.0089E-4
230	0.00199	0.00238	7.4529E-4
235	0.00177	0.00208	6.8121E-4
240	0.00148	0.00171	6.0025E-4
245	0.00113	0.00122	5.1076E-4
250	7.84E-4	8.4681E-4	4.2025E-4
255	4.5796E-4	6.0516E-4	3.2041E-4
260	1.7161E-4	2.7225E-4	2.25E-4
265	4.624E-5	3.136E-5	1.3456E-4
270	2.116E-5	1.21E-6	7.225E-5
275	1.1025E-4	1.1449E-4	2.916E-5
280	3.6864E-4	4.4521E-4	1.936E-5
285	6.9696E-4	7.84E-4	3.249E-5
290	0.00106	0.00116	8.464E-5
295	0.00136	0.00153	1.6641E-4
300	0.00168	0.00189	2.7225E-4
305	0.00194	0.00218	3.7249E-4
310	0.00221	0.00241	4.6656E-4
315	0.00241	0.00272	5.5696E-4
320	0.00264	0.00296	6.4009E-4
325	0.00281	0.00317	7.0756E-4
330	0.00298	0.00333	7.7284E-4
335	0.00312	0.00348	8.2944E-4
340	0.00327	0.00361	8.8209E-4

Continued

A^0	I at $\lambda = 632.8nm$	I at $\lambda = 804.4nm$	I at $\lambda = 808.4nm$
350	0.00343	0.00378	9.4864E-4
345	0.00336	0.00372	9.1204E-4
355	0.00348	0.00382	9.7344E-4
360	0.00354	0.00386	9.9856E-4

Table2. Data of the intensity of reflected light at each analyzer angle for n_y at incident angles $\theta_o = 60.6^0$ for wavelengths $\lambda = 632.8nm$ and $\theta_o = 60.4^0$ $\lambda = 804.4$ and $\lambda = 808.4nm$.

A^0	I at $\lambda = 632.8nm$	I at $\lambda = 804.4nm$	I at $\lambda = 808.4nm$
0	0.00144	0.00108	0.00132
5	0.00143	0.00112	0.00135
10	0.0014	0.00114	0.00135
15	0.00135	0.00115	0.00135
20	0.00129	0.00115	0.00135
25	0.00122	0.00115	0.00134
30	0.00114	0.00114	0.00132
35	0.00104	0.00113	0.00129
40	9.3636E-4	0.00111	0.00126
45	8.2369E-4	0.00107	0.0012
50	6.9169E-4	0.00102	0.00115
55	5.5696E-4	9.7969E-4	0.00108
60	4.1616E-4	9.3025E-4	0.001
65	2.8224E-4	8.41E-4	8.9401E-4
70	1.6129E-4	7.3441E-4	7.6176E-4
75	5.625E-5	6.5536E-4	6.5025E-4
80	1.156E-5	5.8564E-4	5.5696E-4
85	1.6E-7	4.7961E-4	4.2436E-4
90	1.21E-6	3.6864E-4	2.8224E-4

Continued

A^0	I at $\lambda = 632.8nm$	I at $\lambda = 804.4nm$	I at $\lambda = 808.4nm$
95	2.116E-5	2.5921E-4	1.5625E-4
100	8.1E-5	1.44E-4	7.225E-5
105	1.9044E-4	7.396E-5	4.9E-5
110	3.0976E-4	3.481E-5	9.025E-5
115	4.4944E-4	3.481E-5	1.8496E-4
120	5.9536E-4	7.225E-5	3.2761E-4
125	7.3984E-4	1.6384E-4	4.5369E-4
130	8.4681E-4	2.7889E-4	5.9536E-4
135	9.4864E-4	3.8809E-4	7.0225E-4
140	0.00103	4.9729E-4	8.0656E-4
145	0.0011	6.0516E-4	9.1809E-4
150	0.00118	7.0225E-4	0.00101
155	0.00126	7.84E-4	0.00109
160	0.00134	8.7025E-4	0.00115
165	0.00137	9.3025E-4	0.0012
170	0.00141	9.7969E-4	0.00125
175	0.00142	0.00104	0.00129
180	0.00142	0.00108	0.00132
185	0.00141	0.00111	0.00134
190	0.00137	0.00113	0.00135
195	0.00132	0.00114	0.00135
200	0.00126	0.00115	0.00134
205	0.00117	0.00114	0.00132
210	0.00109	0.00114	0.00131
215	9.8596E-4	0.00112	0.00128
220	8.7025E-4	0.0011	0.00125
225	7.5076E-4	0.00107	0.00119

Continued

A^0	I at $\lambda = 632.8nm$	I at $\lambda = 804.4nm$	I at $\lambda = 808.4nm$
230	6.3504E-4	0.00103	0.00113
235	5.1529E-4	9.7969E-4	0.00107
240	3.8809E-4	9.1809E-4	9.8596E-4
245	2.4964E-4	8.4681E-4	9E-4
250	1.3225E-4	7.7284E-4	8.0089E-4
255	4.761E-5	6.8644E-4	6.6564E-4
260	9E-6	5.9536E-4	5.4289E-4
265	1.6E-7	4.8841E-4	4.1616E-4
270	8.1E-7	3.8809E-4	3.0625E-4
275	1.296E-5	2.6569E-4	1.6129E-4
280	6.889E-5	1.5625E-4	7.225E-5
285	1.6384E-4	8.1E-5	4.624E-5
290	3.8809E-4	3.481E-5	8.1E-5
295	4.1209E-4	3.364E-5	1.7956E-4
300	5.5696E-4	7.225E-5	3.1684E-4
305	7.0225E-4	1.6129E-4	4.4944E-4
310	8.2369E-4	2.6896E-4	5.9536E-4
315	9.3636E-4	3.8809E-4	7.1289E-4
320	0.00104	4.9729E-4	8.2369E-4
325	0.00113	6.1009E-4	9.1809E-4
330	0.00121	6.9696E-4	0.001
335	0.00127	7.8961E-4	0.0011
340	0.00134	8.7025E-4	0.00116
345	0.00137	9.1809E-4	0.0012
350	0.0014	9.6721E-4	0.00125
355	0.00141	0.00102	0.00127
360	0.00141	0.00109	0.00133

4.3 Dispersion

When a beam of electromagnetic radiation is propagated in a material medium, its velocity is less than that in vacuum and its intensity gradually decreases as it advances into the medium. The velocity of electromagnetic radiations in a material medium varies with wavelength due to variation of R.I of medium with wavelength. The phenomenon of variation of R.I with wavelength is called *dispersion.* Mathematically it is represented by $dn/d\lambda$. In general the R.I decreases with wavelength. This effect is known as *normal dispersion.* But over small wavelength ranges, there is often increase of R.I due to an increased absorption of the radiation passing through the medium. This effect is known as *anomalous dispersion.* [9] The characteristics of normal dispersion are: (i) the R.I decreases as wavelength increases, (ii) the rate of increase of R.I with wavelength; i.e., $dn/d\lambda$ is greater at shorter wavelengths. In

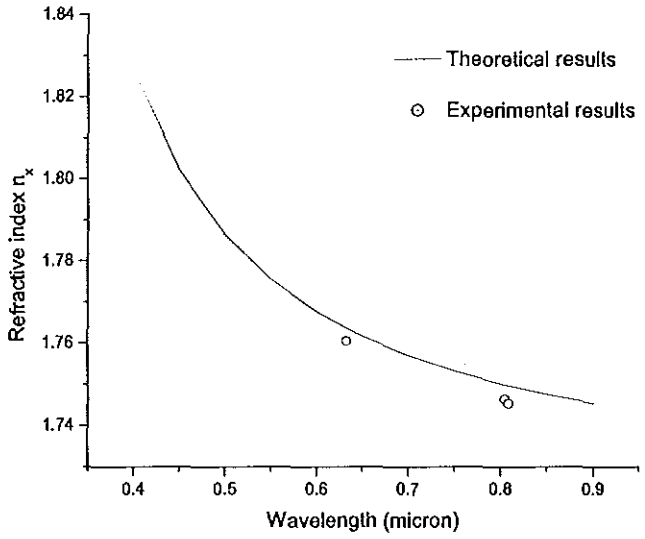

Figure 4.8: *Dispersion graph of KTP crystal for* n_x.

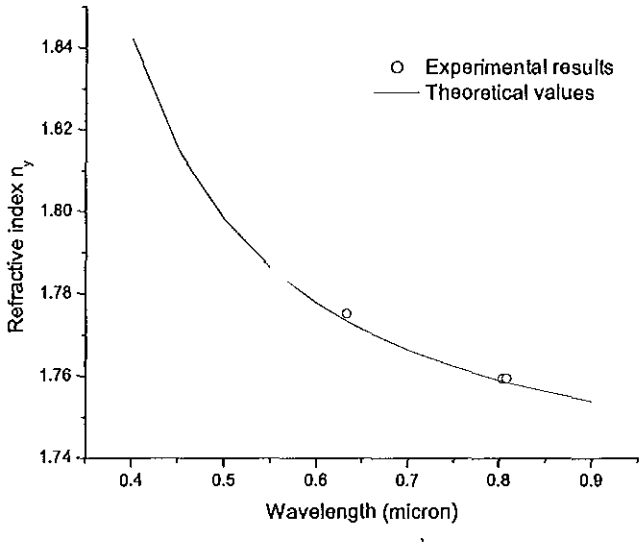

Figure 4.9: *Dispersion graph of KTP crystal for n_y.*

other words dispersion increases as wavelength decreases.

Figures 4.8 and 4.9 show dispersions (n verses λ) graphs of KTP crystal along its x- and y-axis, respectively. The smooth lines are the theoretical expectations and the dots indicate our experimental results. The R.I of KTP crystal decreases with wavelength, which is normal dispersion for KTP crystal.

4.4 Error Analysis

A measured physical quantity, say q, is often used to calculate another physical quautity, $r = f(q)$, from it. Inserting the value of q yields the value of r as we did it in §4.1 to calculate n. An error δq in q produces an error δr in r: "the error in q propagates into r". Since errors are small deviations from the "true" value, we may

use the Taylor expansion to find these propagated errors.

$$\delta r = f(q+\delta q) - f(q) = f'(q)\delta q + \frac{f''(q)}{2!}(\delta q)^2 + \frac{f'''}{3!}(\delta q)^3 + ... \tag{4.4.1}$$

If we make a first-order approximation then the absolute error in r is

$$\delta r = |f'(q)|\delta q. \tag{4.4.2}$$

When $f(q)$ and $f'(q)$ have important common factors, it is useful to calculate the relative error:

$$\frac{\delta r}{|r|} = |\frac{f'(q)}{f(q)}|\delta q. \tag{4.4.3}$$

In our expression the errors $\delta\alpha$ and $\delta\beta$ result in errors in $\tan\Psi$ and $\cos\Delta$,which in turn result in errors in ρ and n. Using Eq. (4.2.2)

$$\delta(\tan\Psi) = \frac{1}{(1+\alpha)^2}\sqrt{\frac{1+\alpha}{1-\alpha}}\tan p\delta\alpha \tag{4.4.4}$$

$$\delta(\cos\Delta) = \frac{\delta\beta}{\sqrt{1-\alpha^2}} + \frac{\alpha\beta}{(1-\alpha^2)^{3/2}}\delta\alpha. \tag{4.4.5}$$

Since

$$\rho = \tan\Psi\cos\Delta,$$

the expression for the absolute error $\delta\rho$ in ρ is

$$|\delta\rho| = \frac{\cos\Delta}{(1+\alpha)^2}\sqrt{\frac{1+\alpha}{1-\alpha}}(\tan P)\delta\alpha + (\frac{\delta\beta}{\sqrt{1-\alpha^2}} + \frac{\alpha\beta}{(1-\alpha^2)^{3/2}}\delta\alpha)\tan\Psi. \tag{4.4.6}$$

This results in the R.I n to have absolute error δn given by

$$|\delta n| = \frac{2\sin\theta_o\tan^2\theta_o}{\sqrt{(1+\rho)^2+(1-\rho)^2\tan^2\theta_o}}\frac{1-\rho}{(1+\rho)^2}|\delta\rho|. \tag{4.4.7}$$

Using the Eqs. (4.3.4) up to (4.3.7), the errors are analyzed and the results of the R.I along with their errors are put in table 3.

Table 3 Refractive index with respective errors at each wavelength.

$\lambda(nm)$	n_x	n_y	δn_x	δn_y	Δn_{xr}	Δn_{yr}
632.8	1.7605	1.7751	4.0062E-5	1.7332E-5	0.0017	0.001
804.4	1.7464	1.7594	5.0081E-5	5.0038E-5	0.00205	0.00034
808.8	1.7454	1.7595	9.9956E-6	1.9995E-5	0.0024	0.00028

where Δn_{xr} and Δn_{yr} denote the relative errors for n_x and n_y, respectively.

Chapter 5

SUMMARY AND CONCLUSIONS

5.1 Summary

A simple reflection ellipsometry technique can be used routinely to evaluate the refractive index (R.I) of NLO materials. We employed this technique to study the linear R.I of KTP crystal. In fact, as a nonlinear material the R.I of KTP crystal includes second order and higher terms for more accuracy. But here we study the linear R.I for the following reasons: (1) the study is carried out in the middle range of its transmission region (i.e., from $632.8nm$ to $808.4nm$) so that absorption and other optical effects do not occur. (2) the intensity of the laser is much less than what is required to produce second harmonic generation and other nonlinear effects. Thus due to these reasons our results are very close to the theoretical values and are not affected by the nonlinearity of the crystal. The R.I obtained in this study is very close to the theoretical values with relative errors up to 0.17 o/o for the n_x and 0.028 o/o for the n_y. As linear R.Is, n_x and n_y of the KTP crystal also show normal dispersion in its transmission range.

5.2 Conclusions

We have employed a simple reflection ellipsometry technique which is nondestructive and sensitive to measure the changes in the state of polarization of light wave of wavelength up to $808.4nm$ for the measurement of the R.I of KTP crystal. We have derived simple relations that allow the R.I to be obtained directly from computer curve fits. For the validity of this technique, we have applied three wavelengths: one visible light wavelength of $\lambda = 632.8nm$ of He-Ne laser source, and the other two, $\lambda = 804.4nm$ and $\lambda = 808.4nm$, from a temperature tuned Semiconductor: Diode laser source. The results obtained in this technique are in good agreement with those obtained in other methods. As a simple and nondestructive method, reflection ellipsometry technique is a preferable one for in situ study. As our study show the precision of 4.0062×10^{-5} to 9.9956×10^{-6} can be obtained for the simple reflection ellipsometry technique. In addition to its precision, ellipsometry (reflection ellipsometry) is a non-invasive and non-destructive tool which can be easily assembled in small laboratories. Moreover, the technique requires only a low-power light source and, consequently, it does not affect most processes, which renders the technique to be a convenient tool for *in situ* studies. The assembled ellipsometry apparatus costs up to $100,000$ USD. But here we assembled the technique in the Optical Laboratory, and proved the validity of the technique. We also hope that this assembled technique can further be developed for future studies to carry on in the University and the Country at large.

Finally, we would like to give a remark to the readers that this thesis presents the basic concepts and applications of ellipsometry technique for the determination of the optical constants of KTP crystal. The descriptions of models and results are in a simplified form, but the readers can find more details about theoretical and experimental parts in the cited references.

Bibliography

[1] Azzam R.M.A., Bashara N.M, (1987) *Ellipsometry and Polarized Light*: In Reflection and Transmission of Polarized light by Stratified Planar Structure. 2^{nd} edn., Elsevier: Amsterdam.

[2] J.D. Bierlein and C.B. Arweiler. (1986) *Electro-optic and dielectric properties of* $KTiOPO_4$. Appl. Phys. Lett, 49, 917 .

[3] G.C. Bhar, A.M. Rudra, U. Chatterjee and A.K. Chaudhary. (1997) *Generation of widely tunable mid-infrared radiation by difference frequency mixing in KTP.* J.Phys. D: Appl. Phys. 30,pp.2693 – 2697, U.K.

[4] G.C. Bhar, A.M. Rudra, A.K. Chaudhary, T.Sasaki and Y.Mori. (1996) *High efficient difference frequency generation in KTP.* Appl.Phys.B. 63, 141 – 144 Germany.

[5] P. Khumbhakar, A.K. Chaudhary, U. Chatterjee. (2000) *A Tunable laser by down conversion in KTP.* Indian J.Phys. Vol. 74A, 119, India.

[6] A.K. Chaudhary, P. Khumbhakar, G.C. Bhar and U.Chatterjee. (2003) *Proceeding of the National Laser Symposium*, I.I.T. Kharagpur, India.

[7] J.Q. Yao and T.S. Fahlen. (1984) *Calculation of optimum phase match parameters for the biaxial crystal* $KTiOPO_4$. J.Appl. Phys. 55, 65.

[8] The Ellipsometer. http://ece-www.colorado.edu/ bart/book/ellipsom.htm.

[9] Satya Prakash. (1994 – 95) *Electromagnetic Theory and Electrodynamics*, 8^{th} edn. Kedar Nath Ram Nath co. India. pp. 441.

[10] Debora Goncalves and E.A. Irene. (2002) *Fundamentals and Applications of Spectroscopic Ellipsometry.* Quimica Nova Vol.25, No.5, Sao Paulo .

[11] Grant R. Fowlers. (1975) *Introduction to Modern Optics.* In Optics of Solids 2^{nd} edn. Holt, Rinehart and Winston, INC. pp. 153 – 175.

[12] *Optical Properties of KTP Crystal*; Wabsite: http//www.castech-us.com/casktp.htm

[13] Peter Milonni and Joseph H. Eberly. (1988), *Lasers.* In Classical Dispersion Theory, John Wiley Sons. pp. 59.

[14] Ossi Kimmelma. (2002) *"Laser Frequency Doubling Using A Periodically Poled Nonlinear Crystals ".* M.Sc. Thesis, Helsinki University of Technology, Helsinki, Finland. pp. 17 – 20.

[15] F.C. Zumsteg, J.D. Bierlein, T.E. Gier, $K_xRb1\text{-}xTiOPO_4$ *A new Nonlinear Optical Material*; Journal of Applied Physics, Vol. 47, pp. 4980 – 4985.

[16] Azzam R.M.A., Bashara N.M, (1987) *Ellipsometry and Polarized Light*: In The Polarization of Light waves. 2^{nd} edn., Elsevier: Amsterdam, pp.1 – 16.

[17] Y.S. Liu, L. Drafall, D. Dentz and R. Belt. (1982) *Nonlinear optical-matching properties of* $KTiOPO_4$. Technical Information Series Rep. 82CRD016 (General Electric, Schenectady, N.Y).

[18] Azzam R.M.A., Bashara N.M, (1987) *Ellipsometry and Polarized Light:* In Propagation of Polarized Light through Polarizing Optical Systems. pp. 66 – 71, 77 – 79.

[19] Azzam R.M.A., Bashara N.M, (1987) *Ellipsometry and Polarized Light*: In Theorey and Analysis of Measurements in Ellipsometer Systems. pp 154 – 174.